

# Scalable Bayesian inference for high-dimensional mixed-type multivariate spatial data

Arghya Mukherjee<sup>1</sup>, Arnab Hazra<sup>1</sup>, and Dootika Vats<sup>1</sup>

<sup>1</sup>Indian Institute of Technology Kanpur

## Abstract

Spatial generalized linear mixed-effects methods are popularly used to model spatially indexed univariate responses. However, with modern technology, it is common to observe vector-valued mixed-type responses, e.g., a combination of binary, count, or continuous types, at each location. Methods that allow joint modeling of such mixed-type multivariate spatial responses are rare. Using latent multivariate Gaussian processes (GPs), we present a class of Bayesian spatial methods that can be employed for any combination of exponential family responses. Since multivariate GP-based methods can suffer from computational bottlenecks when the number of spatial locations is high, we further employ a computationally efficient Vecchia approximation for fast posterior inference and prediction. Key theoretical properties of the proposed model, such as identifiability and the structure of the induced covariance, are established. Our approach employs a Markov chain Monte Carlo-based inference method that utilizes elliptical slice sampling in a blocked Metropolis-within-Gibbs sampling framework. We illustrate the efficacy of the proposed method through simulation studies and a real-data application on joint modeling of wildfire counts and burnt areas across the United States.

**Keywords**— Large spatial data analysis, Latent Gaussian process, Mixed-type spatial responses, Multivariate spatial Bayesian modeling, Markov chain Monte Carlo, Vecchia approximation.

## 1 Introduction

In recent years, the scale and ubiquity of vast, spatially indexed datasets have grown significantly. This expansion is largely fueled by technological advancements, such as the

Global Positioning System and Remote Sensing, alongside the relentless growth of digital storage capacities. Spatially indexed responses can be multivariate and more specifically also “mixed-type”, i.e., responses can be a combination of continuous, skewed continuous, binary, count, and other types. In this work, we introduce a simple and interpretable Bayesian model for spatial point-referenced multivariate data that accommodates mixed-type responses from the exponential family.

Flexible statistical modeling and inference for mixed-type spatial data is important due to two types of dependence: (a) spatial dependence across locations, and (b) dependence across different response variables. Understanding the relationship between different types of spatial responses is crucial across numerous scientific domains, including environmental science, epidemiology, and risk assessment. For instance, to improve predictive accuracy in wildfire modeling (Opitz, 2023), one may seek to jointly analyze count-type responses like wildfire frequencies and continuous-type responses like the total burnt area (Cisneros et al., 2023). More broadly, climate scientists may be interested in studying whether incorporating both types of information enhances inference in assessing environmental hazards. Similarly, in public health research, the National Academy of Sciences of the United States has emphasized the importance of monitoring daily fine particulate matter ( $PM_{2.5}$ ) due to its strong association with adverse health outcomes (Burnett et al., 2018). Elevated  $PM_{2.5}$  levels have been linked to increased mortality risks, including lung cancer in individuals with no prior history of smoking (Turner et al., 2011) and heightened cardiovascular mortality (Brook et al., 2010). The interdependency among different responses suggests that jointly modeling  $PM_{2.5}$  concentrations (continuous-type) and disease incidence or mortality counts (discrete-type) could yield more profound insights into their relationships. Our methodological framework aims to address such challenges by providing a flexible and scalable approach for high-dimensional mixed-type spatial data.

Most existing methods for mixed-type response models have been developed for specific applications and are not generally applicable to spatial models. For example, Gueorguieva (2001) proposed joint models for dependent discrete and continuous outcomes in biomedical studies, and Goldstein et al. (2009) extended multilevel models to deal with incomplete and structured data. Generalized linear latent variable models offer a more flexible framework for modeling mixed-type responses (Sammel et al., 1997), including extensions to longitudinal settings (Yang et al., 2014). More recent approaches also account for zero inflation and over-dispersion in continuous and count responses (Kassahun et al., 2015; Molenberghs et al., 2010). Their methods are designed for specific paired combinations of response types, such as continuous and count, or continuous and binary. They are not flexible enough to be

extended to spatially correlated data with various possible types of multi-response data.

We develop a Bayesian hierarchical framework for modeling mixed-type spatial responses. The model flexibly accommodates data comprising different response types by employing a unified latent process structure, allowing joint inference across varied measurement scales. To address the computational challenges inherent in analyzing large spatial datasets, we use the Vecchia approximation (Vecchia, 1988) in our model that significantly reduces the cost of matrix operations typically associated with GPs, making posterior inference via Markov chain Monte Carlo (MCMC) amenable even in high-dimensional spatial settings. The proposed approach is particularly well-suited for applications involving a large number of spatial locations and a moderate number of response variables, which is a common scenario.

The structure of the paper is as follows. Section 2 provides a concise review of spatial multivariate models. Building on this foundation, we highlight key challenges and introduce the core components of our proposed mixed-type multivariate spatial model. We then extend this model to high-dimensional settings by incorporating the Vecchia approximation for improved scalability. In Section 3, we present an MCMC algorithm for scalable Bayesian inference. Section 4 focuses on fast predictive inference, while Section 5 explores the performance of our approach through both simulated and real data analysis. Finally, in Section 6, we summarize our contributions and outline promising directions for future research.

## 2 Methodology

We present the ingredients for a multivariate spatial model that accommodates mixed-type outcomes, briefly review the existing approaches to model multivariate point-referenced spatial data, and subsequently develop our proposed model.

### 2.1 Background

Suppose for each spatial site  $\mathbf{s}$  within a compact domain  $\mathcal{D} \subset \mathbb{R}^d$ , we have a multivariate response  $\mathcal{Y}(\mathbf{s}) = [Y_1(\mathbf{s}), Y_2(\mathbf{s}), \dots, Y_q(\mathbf{s})]^\top$  on  $q$  variables of interest, along with information on spatially varying vector of covariates denoted by  $\mathcal{X}(\mathbf{s}) \in \mathbb{R}^p$ . Classical multivariate spatial models (Zhang et al., 2021) specify all components of  $\mathcal{Y}(\mathbf{s})$  to be continuous and equipped with a latent multivariate zero-mean spatially colored process  $\mathcal{W}(\mathbf{s}) = [W_1(\mathbf{s}), W_2(\mathbf{s}), \dots, W_q(\mathbf{s})]^\top$  such that for different  $j \in \{1, \dots, q\}$ ,  $W_j(\mathbf{s})$  stitches the cross-dependence among the  $q$  outcomes. Each component of  $\mathcal{Y}(\mathbf{s})$  is thus modeled using a spatial

regression model given by

$$Y_j(\mathbf{s}) = \mathcal{X}(\mathbf{s})^\top \boldsymbol{\beta}_j + W_j(\mathbf{s}) + \varepsilon_j(\mathbf{s}), \quad j = 1, 2, \dots, q, \quad (1)$$

where the  $p$ -dimensional regression coefficient corresponding to the covariate  $\mathcal{X}(\mathbf{s})$  for the  $j$ -th response is denoted by  $\boldsymbol{\beta}_j$  and  $\varepsilon_j(\mathbf{s}) \stackrel{\text{iid}}{\sim} \mathcal{N}(0, \tau^2)$  captures measurement error or nugget effect independently of  $\mathbf{s}$ . The dependence structure of the process  $\mathcal{W}(\cdot)$  is specified by a  $q$ -dimensional matrix-valued covariance kernel, denoted as  $\mathbf{C}(\cdot, \cdot)$ . At locations  $\mathbf{s}$  and  $\mathbf{s}'$  in  $\mathcal{D}$ , spatial covariance between the  $i$ -th and  $j$ -th components of the process can be specified by the  $(i, j)$ th element of the matrix-valued covariance function as

$$C_{ij}(\mathbf{s}, \mathbf{s}') = \text{Cov} [W_i(\mathbf{s}), W_j(\mathbf{s}')] \text{ for all } i, j = 1, \dots, q. \quad (2)$$

[Genton and Kleiber \(2015\)](#) review diverse choices of covariance functions of the form compatible with (2), which can yield a flexible class of models discussed in (1). However, such models in (1) assume Gaussian marginals for each  $Y_j(\mathbf{s})$  and do not naturally extend to mixed outcome types.

A major challenge of Bayesian spatial generalized linear mixed-effects models (spGLMMs) in high dimensions lies in posterior sampling, due to the additional complexity of intractable likelihoods ([Christensen and Sköld, 2006](#)). One of the earliest works in this direction is by [Zhu et al. \(2005\)](#), who proposed a frequentist generalized latent variable model for replicated multivariate spatiotemporal data. More recently, conjugate Bayesian models have been introduced for multivariate responses from exponential family distributions using Diaconis–Ylvisaker conjugate priors, which enable MCMC-free inference and thereby offer computational advantages ([Bradley and Clinch, 2025; Nandy et al., 2022; Zhou and Bradley, 2024](#)). However, these methods often impose simplified or fixed spatial dependence structures and may not scale well with increasing numbers of response types or spatial locations.

Some studies use copula-based models to capture dependence in mixed-type responses ([de Leon and Wu, 2011; Fitzmaurice and Laird, 1995; Song et al., 2009](#)). While useful, copulas do not uniquely specify the marginal dependence with discrete outcomes, and computation is challenging in high-dimensional spatial models ([Hazra and Huser, 2021; Hazra et al., 2024](#)). In contrast, hierarchical models offer a more tractable way to jointly model marginal distributions with an explainable dependence structure. In the non-spatial setting, mixed-type response models have been studied using latent factor models ([Jiryaei et al., 2016](#)), or multivariate generalized linear models ([Ekvall and Molstad, 2022](#)) that

link each response to its own linear predictor. While these methods are effective for small-scale and non-spatial problems, they often struggle with computational scalability in high dimensions. The sparse scientific studies in the spatial statistics community have led us to develop a simple yet useful Bayesian hierarchical model that can jointly handle mixed-type responses and spatial dependence within a coherent latent variable framework.

## 2.2 Proposed joint model

For any arbitrary spatial location  $\mathbf{s} \in \mathcal{D}$ , let the  $q$ -variate mixed-type response vector be  $\mathcal{Y}(\mathbf{s}) = [Y_1(\mathbf{s}), \dots, Y_q(\mathbf{s})]^\top$  with a latent multivariate process  $\mathcal{W}(\mathbf{s}) = [W_1(\mathbf{s}), \dots, W_q(\mathbf{s})]^\top$ . For each  $j = 1, \dots, q$  and  $\mathbf{s} \in \mathcal{D}$ , we model  $Y_j(\mathbf{s})$  as conditionally independent given  $W_j(\mathbf{s})$ . We specify a known canonical link function  $g_j$  for each  $j$ -th response type, according to [Diggle et al. \(1998\)](#) and define the conditional mean of  $Y_j(\mathbf{s})$  through

$$g_j(\mathbf{E}[Y_j(\mathbf{s}) \mid W_j(\mathbf{s})]) = W_j(\mathbf{s}). \quad (3)$$

Let the cumulant function be denoted by  $b_j(\cdot)$  and the known dispersion parameter associated with the  $j$ -th response be  $\psi_j$ . We assume  $Y_j(\mathbf{s})$  follows an exponential family distribution, denoted by  $\text{EF}(Y_j(\mathbf{s}) \mid W_j(\mathbf{s}) = w, \psi_j)$ , with a Lebesgue or count measure dominated density, evaluated at  $y$  as

$$f_j(y \mid w, \psi_j) = h(y, \psi_j) \exp \left[ \frac{yw - b_j(w)}{\psi_j} \right]. \quad (4)$$

We adopt a centered parameterization proposed by [Christensen and Sköld \(2006\)](#) for the latent multivariate process  $\mathcal{W}(\cdot) = [W_1(\cdot), \dots, W_q(\cdot)]^\top$  and assume

$$\mathcal{W}(\cdot) \sim \mathcal{GP}_q \left( \mathbf{B}^\top \mathcal{X}(\cdot), \mathbf{C}(\cdot, \cdot) \right), \quad (5)$$

where  $\mathbf{B} = (\boldsymbol{\beta}_1, \dots, \boldsymbol{\beta}_q) \in \mathbb{R}^{p \times q}$  denotes the regression coefficient matrix with each element  $(\boldsymbol{\beta}_{ij})_{1 \leq i \leq p, 1 \leq j \leq q}$  being the fixed effect corresponding to the  $i$ -th covariate and  $j$ -th response,  $\mathcal{GP}_q$  denotes a  $q$ -variate GP, and  $\mathbf{C}(\cdot, \cdot)$  is the multivariate covariance kernel. To enable efficient computation and parsimonious inference on the covariance function, we impose a separable structure

$$\mathbf{C}(\mathbf{s}, \mathbf{s}') = \mathcal{K}(\mathbf{s}, \mathbf{s}') \boldsymbol{\Sigma}, \quad \mathbf{s}, \mathbf{s}' \in \mathcal{D}, \quad (6)$$

where  $\boldsymbol{\Sigma} = (\boldsymbol{\Sigma}_{ij})_{1 \leq i, j \leq q}$  is a  $q \times q$ -dimensional spatially-invariant matrix that captures cross-response covariance, and  $\mathcal{K}(\mathbf{s}, \mathbf{s}')$  is a valid univariate spatial correlation function. We

use the commonly used Matérn kernel (Matérn, 1960) as a flexible choice for  $\mathcal{K}$  given by

$$\mathcal{K}(\mathbf{s}, \mathbf{s}') = \frac{1}{2^{\nu-1}\Gamma(\nu)} \left( \frac{\|\mathbf{s} - \mathbf{s}'\|_2}{\phi} \right)^\nu K_\nu \left( \frac{\|\mathbf{s} - \mathbf{s}'\|_2}{\phi} \right), \quad \phi > 0, \nu > 0, \quad (7)$$

where  $K_\nu$  is the modified Bessel function of the second kind. Here, the parameter  $\phi$  controls the range of spatial dependence, and the smoothness parameter  $\nu$ , which we assume to be fixed, determines the smoothness of the process. Hereafter, we denote the Matérn kernel  $\mathcal{K}$  in (7) as  $\mathcal{K}_\phi$  with parameter  $\phi$ .

Before introducing our joint model, we define the parameters and describe prior specifications used in our proposed Bayesian framework. Conditioning on the  $q \times q$  response cross-covariance matrix  $\Sigma$ , we specify a Matrix-Normal prior on the  $p \times q$ -dimensional regression coefficient matrix  $\mathbf{B}$ , denoted by  $\mathcal{MN}_{p,q}$ , given by  $\mathbf{B} | \Sigma \sim \mathcal{MN}_{p,q}(\mathbf{M}, \mathbf{V}, \Sigma)$ . Here  $\mathbf{M}$  is a  $p \times q$  mean matrix and  $\mathbf{V}$  is a  $p \times p$  dimensional positive definite matrix expressing the row-wise covariance matrix of  $\mathbf{B}$ . The prior distribution of  $\mathbf{B}$  depends on the data-level covariance matrix  $\Sigma$ . While we can specify this prior covariance to be different from  $\Sigma$  with a different matrix of the same dimension, it would drastically increase the computational burden (Hazra et al., 2020). For the cross-response covariance matrix  $\Sigma$ , we adopt a commonly used Inverse-Wishart prior  $\Sigma \sim \mathcal{IW}(\mathbf{S}, v)$ , with a positive definite scale matrix  $\mathbf{S}$  and degrees of freedom  $v$ . The spatial correlation is governed by a Matérn kernel in (7) with  $\phi$  and  $\nu$ . Since consistent estimation of the Matérn parameters is challenging (Zhang, 2004), we fix  $\nu$  at a reasonable value and assign a uniform prior for  $\phi$  as  $\phi \sim \mathcal{U}(0, b_\phi)$ , where  $b_\phi$  is chosen so that the effective range corresponds to a minimal correlation (say, 0.01 or 0.05) at the domain diameter  $\Delta = \max_{i,j} \|\mathbf{s}_i - \mathbf{s}_j\|_2$ , ensuring sufficient posterior learning through data. We will discuss the reasoning for the prior of  $\phi$  in Section 3. We further assume that the conditional cumulant functions  $b_j(\cdot)$  for one-parameter regular exponential families are strictly convex for the  $j$ -th response. Consequently, defining the data and priors, our proposed hierarchical model is

$$\begin{aligned} \text{Data level: } & Y_j(\mathbf{s}) | W_j(\mathbf{s}) \stackrel{\text{ind}}{\sim} \text{EF}(Y_j(\mathbf{s}) | W_j(\mathbf{s}), \psi_j), \quad j = 1, \dots, q, \quad \mathbf{s} \in \mathcal{D}, \\ \text{Process level: } & \mathcal{W}(\cdot) | \mathbf{B}, \Sigma, \phi \sim \mathcal{GP}_q(\mathbf{B}^\top \mathcal{X}(\cdot), \mathcal{K}_\phi(\cdot, \cdot) \Sigma), \\ \text{Parameter level: } & \mathbf{B} | \Sigma \sim \mathcal{MN}_{p,q}(\mathbf{M}, \mathbf{V}, \Sigma), \\ & \Sigma \sim \mathcal{IW}(\mathbf{S}, v), \\ & \phi \sim \mathcal{U}(0, b_\phi). \end{aligned} \quad (8)$$

Our proposed conditional model allows flexibility of modeling dependence through the latent

variable structure while allowing the conditional likelihood function to be any member of the exponential family. Moreover, we provide a rich class of Matrix-Normal Inverse-Wishart (MNIW) prior on  $(\mathbf{B}, \Sigma)$ , which is widely used in multi-response regression analysis (Zhang et al., 2021). Besides, the spatial range parameter  $\phi$  is assigned a uniform prior to ensure flexibility in spatial correlation over the domain.

We observe the data at  $n$  spatial locations  $\mathcal{S} = \{\mathbf{s}_1, \dots, \mathbf{s}_n\} \subset \mathcal{D}$ , where each site leads to a  $q$ -variate response  $\mathcal{Y}(\mathbf{s}_i) \in \mathbb{R}^q$  and covariates  $\mathcal{X}(\mathbf{s}_i) \in \mathbb{R}^p$ . The stacked observed response matrix, the latent spatial random effects matrix, and the covariate matrix, respectively, are

$$\mathbf{Y} = \begin{bmatrix} \mathcal{Y}(\mathbf{s}_1)^\top \\ \mathcal{Y}(\mathbf{s}_2)^\top \\ \vdots \\ \mathcal{Y}(\mathbf{s}_n)^\top \end{bmatrix}_{n \times q}, \quad \mathbf{W} = \begin{bmatrix} \mathcal{W}(\mathbf{s}_1)^\top \\ \mathcal{W}(\mathbf{s}_2)^\top \\ \vdots \\ \mathcal{W}(\mathbf{s}_n)^\top \end{bmatrix}_{n \times q}, \quad \mathbf{X} = \begin{bmatrix} \mathcal{X}(\mathbf{s}_1)^\top \\ \mathcal{X}(\mathbf{s}_2)^\top \\ \vdots \\ \mathcal{X}(\mathbf{s}_n)^\top \end{bmatrix}_{n \times p}.$$

Under the separable covariance  $\mathbf{C}(\mathbf{s}, \mathbf{s}') = \mathcal{K}_\phi(\mathbf{s}, \mathbf{s}')\Sigma$ , the induced covariance of the vectorized latent process, denoted as  $\text{vec}(\mathbf{W})$  across all spatial sites is  $\boldsymbol{\Omega}_\phi := \Sigma \otimes \mathbf{K}_\phi$ , where  $\mathbf{K}_\phi = (\mathcal{K}_\phi(\mathbf{s}_i, \mathbf{s}_j))_{1 \leq i, j \leq n}$ . The  $\text{vec}(\cdot)$  operator transforms a matrix into a column vector by vertically stacking the columns of the matrix. The latent matrix  $\mathbf{W}$  thus follows a Matrix-Normal distribution specified as

$$\mathbf{W} \mid \mathbf{B}, \Sigma, \phi \sim \mathcal{MN}_{n,q}(\mathbf{X}\mathbf{B}, \mathbf{K}_\phi, \Sigma) \iff \text{vec}(\mathbf{W}) \mid \mathbf{B}, \Sigma, \phi \sim \mathcal{N}_{nq}((\mathbf{I}_q \otimes \mathbf{X}) \text{vec}(\mathbf{B}), \boldsymbol{\Omega}_\phi). \quad (9)$$

We assume that the underlying data over  $\mathcal{S}$  is generated from our proposed model in (8). To be specific, each column of  $\mathbf{Y}$  is conditionally independent of the corresponding columns of  $\mathbf{W}$ . We demonstrate our hierarchical model on observed datasets with a directed acyclic graph in Figure 1.

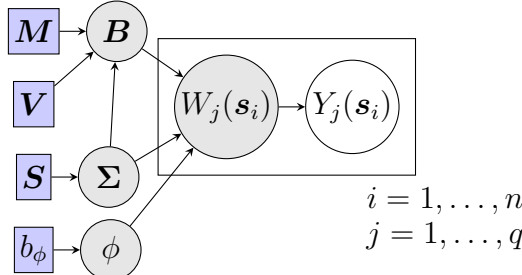


**Figure 1:** Directed acyclic graph representation of our model.

## 2.3 Model properties

We discuss properties of our model that are essential for reliable posterior inference. Although the simple structure of our proposed model facilitates interpretability, it also raises concerns about potential misspecification and its impact on inference. In the context of spatial mixed-type response models, this typically involves selecting a parameterized covariance structure for the random effects. However, even with a well-specified, non-overparameterized, and separable covariance matrix for the responses, models for data with non-replicated observations may still suffer from non-identifiability (Zhang, 2004). We discuss some model properties using the marginal mean and covariance of  $\text{vec}(\mathbf{Y})$ . Denoting  $\mathbf{g} = (g_1, g_2, \dots, g_q)^\top$  to be the vectorized link function corresponding to  $q$ -types of responses, we write

$$\mathbb{E}[\text{vec}(\mathbf{Y})] = \mathbf{g}^{-1}(\text{vec}(\mathbf{W})), \quad \text{cov}[\text{vec}(\mathbf{Y})] = \text{cov}[\mathbf{g}^{-1}(\text{vec}(\mathbf{W}))] + \mathbb{E}[\text{cov}[\text{vec}(\mathbf{Y}) \mid \text{vec}(\mathbf{W})]]. \quad (10)$$

From (10), several observations follow. For any  $k \in \{1, 2, \dots, q\}$ , we define  $b_k''(\cdot)$  to be the second derivative of the cumulant function. We can write the conditional covariance as

$$\text{cov}[\text{vec}(\mathbf{Y}) \mid \text{vec}(\mathbf{W})] = \text{block-diag}(\mathbf{A}_1, \dots, \mathbf{A}_q) \text{ with } \mathbf{A}_k = \psi_k \text{ diag} \left( \mathbb{E}[b_k''(W_k(\mathbf{s}_i))] \right)_{1 \leq i \leq n},$$

which is block-diagonal and the cross-dependence across the  $q$  responses is determined by  $\text{cov}[\mathbf{g}^{-1}(\text{vec}(\mathbf{W}))]$ . Due to having different dispersion parameters  $\psi_k$  and cumulant functions  $b_k$ , the block-diagonal matrices  $\mathbf{A}_k$  are thus distinct for  $q$ -different responses. Hence,  $\text{cov}[\text{vec}(\mathbf{Y}) \mid \text{vec}(\mathbf{W})]$  exhibits a non-separable covariance structure. This implies that, even though a separable covariance is assumed for the latent matrix  $\mathbf{W}$ , the marginal covariance of  $\mathbf{Y}$  can still be non-separable and spatially varying. As a result, our model retains the flexibility to capture heterogeneous covariance both across response types and over space. Second, for any spatial location  $\mathbf{s}$ , the univariate distribution of  $Y_j$  fully determines both  $\mathbb{E}[Y_j(\mathbf{s})]$  and  $\mathbb{E}[Y_j^2(\mathbf{s})]$  and consequently it directly follows that the off-diagonal elements of  $\Sigma$  do not influence the marginal means or variances. Their contribution is restricted to the dependence structure across locations. Therefore, the marginal variability coincides with that obtained from a model in which  $\Sigma_{ij} = 0$  for  $i \neq j$ . Third, since  $\mathbf{g}$  and  $\text{cov}[\text{vec}(\mathbf{Y}) \mid \text{vec}(\mathbf{W})]$  are generally nonlinear and non-constant (for example  $\mathbf{g}$  can be a vectorized function of logit, log-link, etc.), both  $\mathbb{E}[\text{vec}(\mathbf{Y})]$  and  $\mathbb{E}[\text{cov}[\text{vec}(\mathbf{Y}) \mid \text{vec}(\mathbf{W})]]$  depend on  $\boldsymbol{\beta}$  and the diagonal elements of  $\Sigma$ . Fourth, because  $\text{var}[Y_j(\mathbf{s})] = \psi_j \mathbb{E}[b_j''(W_j(\mathbf{s}))]$  increases with  $\psi_j$  while  $\text{cov}[\mathbf{g}^{-1}(\text{vec}(\mathbf{W}))]$  is independent of  $\boldsymbol{\psi} = (\psi_1, \dots, \psi_q)$ , for any two

locations  $\mathbf{s}$  and  $\mathbf{s}'$ , the magnitude of correlation  $\text{corr}[Y_j(\mathbf{s}), Y_k(\mathbf{s}')]$  decreases as  $\psi_j$  or  $\psi_k$  increase. Intuitively, since different response types are conditionally uncorrelated, a large  $\psi_j$  indicates that much of the variation in  $Y_j(\mathbf{s})$  is independent of variation in the other responses. We provide a general definition of weak identifiability of the model parameters as given in [Ekvall and Molstad \(2022\)](#) and derive some results that establish some key theoretical properties of our model.

**Definition 1.** Suppose a model  $\mathcal{P}_\gamma = \{F_\gamma : \gamma \in \Gamma\}$  is a class of distribution functions  $F_\gamma$  parameterized by  $\gamma \in \Gamma \subseteq \mathbb{R}^r$ . Then  $\mathcal{P}_\gamma$  is said to be weakly identifiable for any component of  $\gamma$  with size  $k$ , say  $\gamma_k : k \in \{1, 2, \dots, d\}$  if the mapping  $\gamma_k \rightarrow F_{\gamma_k}$  is injective.

Definition 1 means that two distinct subsets of  $\gamma_k : k \in \{1, 2, \dots, d\}$  should identify two different probability distributions i.e, if  $\gamma_k \neq \gamma_k^*$  then  $F_{\gamma_k} \neq F_{\gamma_k^*}$ . The non-identifiable parameters often result in inconsistent estimation. Our model on observed locations  $\mathcal{S}$  is parameterized by  $[\text{vec}(\mathbf{W})^\top, \text{vec}(\mathbf{B})^\top, \text{vec}(\boldsymbol{\Sigma})^\top, \phi]^\top \in \mathbb{R}^r$  with dimension  $r = nq + pq + q(q+1)/2 + 1$ . This clearly dominates the dimension of data of size  $nq$ , so parameter identifiability plays an important role in our analysis. We provide a result on the non-identifiability of the variance component for Bernoulli responses with a logit link.

**Theorem 2.** In our proposed mixed-type spatial model described in (8) with  $q \geq 1$  responses, suppose the  $j$ -th response type is Bernoulli with a logit link. Then, model parameters are identifiable if  $\boldsymbol{\Sigma}_{jj}$  is assumed to be fixed.

*Proof.* The proof is along with the lines of [Ekvall and Molstad \(2022, Theorem 1\)](#). Suppose we fix a location  $\mathbf{s} \in \mathcal{D}$ . For the  $j$ -th response,

$$Y_j(\mathbf{s}) \mid W_j(\mathbf{s}) \stackrel{\text{ind}}{\sim} \text{Ber} \left( \frac{1}{1 + \exp\{-W_j(\mathbf{s})\}} \right).$$

Here,  $W_j(\mathbf{s}) \sim \mathcal{N}(\mathcal{X}(\mathbf{s})^\top \boldsymbol{\beta}_j, \boldsymbol{\Sigma}_{jj})$  with  $\boldsymbol{\beta}_j$  denoting the regression coefficient vector corresponding to the  $j$ -th type response of length  $p$ . The marginal expectation of  $Y_j(\mathbf{s})$  is

$$\mathbb{E}[Y_j(\mathbf{s})] = \mathbb{E}_{W_j(\mathbf{s})} [\mathbb{E}[Y_j(\mathbf{s}) \mid W_j(\mathbf{s})]] = \int_{\mathbb{R}} \frac{1}{1 + \exp\{-w\}} \pi(w) dw.$$

Here,  $\pi(w)$  denotes the density of  $W_j(\mathbf{s})$  evaluated at  $w$ . Under the model assumptions, we may write

$$W_j(\mathbf{s}) = \mathcal{X}(\mathbf{s})^\top \boldsymbol{\beta}_j + \sqrt{\boldsymbol{\Sigma}_{jj}} Z, \quad \text{with } Z \sim \mathcal{N}(0, 1).$$

After a change of variables, the marginal success probability can be expressed as

$$E[Y_j(\mathbf{s})] = \int_{\mathbb{R}} \frac{1}{1 + \exp\{-\mathcal{X}(\mathbf{s})^\top \boldsymbol{\beta}_j - \sqrt{\boldsymbol{\Sigma}_{jj}}z\}} \varphi(z) dz,$$

where  $\varphi(z)$  is the density of a standard normal distribution evaluated at  $z$ . Fixing all among  $p$  coordinates of  $\mathcal{X}(\mathbf{s})$  except one, say the  $k$ th coordinate, and denoting  $\boldsymbol{\beta}_{jk}$  the corresponding regression coefficient, we obtain the marginal success probability as a function of  $(\boldsymbol{\beta}_{jk}, \boldsymbol{\Sigma}_{jj})$  as

$$\delta(\boldsymbol{\beta}_{jk}; \boldsymbol{\Sigma}_{jj}) := E[Y_j(\mathbf{s})] = \int_{\mathbb{R}} \frac{1}{1 + \exp\left\{-\sum_{l=1(\neq k)}^p x_l(\mathbf{s})\boldsymbol{\beta}_{jl} - \boldsymbol{\beta}_{jk}x_k(\mathbf{s}) - \sqrt{\boldsymbol{\Sigma}_{jj}}z\right\}} \varphi(z) dz. \quad (11)$$

Here,  $\sum_{l=1(\neq k)}^p x_l(\mathbf{s})\boldsymbol{\beta}_{jl}$  denotes the contribution of fixed effects except from the  $k$ th component of  $\mathcal{X}(\mathbf{s})$ . Without loss of generality, let  $x_k(\mathbf{s}) > 0$  for the argument below. Our assumption is valid as our model includes an intercept term for which at least  $x_1(\mathbf{s}) = 1$ . The inverse-logit function  $u \mapsto g(u) := (1 + \exp\{-u\})^{-1}$  is smooth and strictly increasing with derivative  $g'(u) = g(u)\{1 - g(u)\} > 0$ . Differentiating with respect to  $\boldsymbol{\beta}_{jk}$  in (11) under the integral sign (justified by dominated convergence since  $0 < g(\cdot) < 1$ ) yields

$$\begin{aligned} \frac{\partial}{\partial \boldsymbol{\beta}_{jk}} \delta(\boldsymbol{\beta}_{jk}; \boldsymbol{\Sigma}_{jj}) &= \int_{\mathbb{R}} g'\left(\sum_{l=1(\neq k)}^p x_l(\mathbf{s})\boldsymbol{\beta}_{jl} + \boldsymbol{\beta}_{jk}x_k(\mathbf{s}) + \sqrt{\boldsymbol{\Sigma}_{jj}}z\right) x_k \varphi(z) dz \\ &= x_k \int_{\mathbb{R}} g\left(\sum_{l=1(\neq k)}^p x_l(\mathbf{s})\boldsymbol{\beta}_{jl} + \boldsymbol{\beta}_{jk}x_k(\mathbf{s}) + \sqrt{\boldsymbol{\Sigma}_{jj}}z\right) \\ &\quad \times \{1 - g\left(\sum_{l=1(\neq k)}^p x_l(\mathbf{s})\boldsymbol{\beta}_{jl} + \boldsymbol{\beta}_{jk}x_k(\mathbf{s}) + \sqrt{\boldsymbol{\Sigma}_{jj}}z\right)\} \varphi(z) dz. \end{aligned}$$

Because  $x_k > 0$  and  $g'(u) > 0$ , for all  $u \in \mathbb{R}$ , we have  $\frac{\partial}{\partial \boldsymbol{\beta}_{jk}} \delta(\boldsymbol{\beta}_{jk}; \boldsymbol{\Sigma}_{jj}) > 0$ , so  $\delta(\cdot; \boldsymbol{\Sigma}_{jj})$  is strictly increasing and continuous in  $\boldsymbol{\beta}_{jk}$  for each fixed  $\boldsymbol{\Sigma}_{jj}$ . We next evaluate the limits of  $\delta(\boldsymbol{\beta}_{jk}; \boldsymbol{\Sigma}_{jj})$  as  $\boldsymbol{\beta}_{jk} \rightarrow \pm\infty$ . For any fixed  $\mathbf{z}$ ,

$$\lim_{\boldsymbol{\beta}_{jk} \rightarrow -\infty} g\left(\sum_{l=1(\neq k)}^p x_l(\mathbf{s})\boldsymbol{\beta}_{jl} + \boldsymbol{\beta}_{jk}x_k(\mathbf{s}) + \sqrt{\boldsymbol{\Sigma}_{jj}}z\right) = 0, \text{ and}$$

$$\lim_{\beta_{jk} \rightarrow +\infty} g \left( \sum_{l=1(\neq k)}^p x_l(\mathbf{s}) \beta_{jl} + \beta_{jk} x_k(\mathbf{s}) + \sqrt{\Sigma_{jj}} z \right) = 1.$$

Since  $Z$  is integrable, dominated convergence yields

$$\lim_{\beta_{jk} \rightarrow -\infty} \delta(\beta_{jk}; \Sigma_{jj}) = 0, \quad \lim_{\beta_{jk} \rightarrow +\infty} \delta(\beta_{jk}; \Sigma_{jj}) = 1.$$

To prove non-identifiability of  $\Sigma_{jj}$  we now fix two particular values of  $\Sigma_{jj}$  such that  $\Sigma_{jj}^{(1)} \neq \Sigma_{jj}^{(2)}$ . By the continuity and strict monotonicity of  $\beta_{jk} \mapsto \delta(\beta_{jk}; \Sigma_{jj})$ , for an unique  $\beta_{jk}$ , the model can admit the same marginal probability  $p_0 := f(\beta_{jk}; \Sigma_{jj}^{(i)}) \in (0, 1)$  for  $i = 1, 2$  and its limits 0 and 1 when  $\beta_{jk} \rightarrow \pm\infty$ . Thus,  $(\beta_{jk}, \Sigma_{jj}^{(1)})$  distinct from  $(\beta_{jk}, \Sigma_{jj}^{(2)})$  yield the same marginal success probability  $p_0$  at location  $\mathbf{s}$ . Hence,  $\delta$  is not an injective function of  $\Sigma_{jj}$  and thus not identifiable in  $\Sigma_{jj}$ .  $\square$

Theorem 2 directly shows that different values of  $\Sigma_{jj}$  lead to identical marginal Bernoulli probabilities at location  $\mathbf{s}$ . Consequently, without an additional constraint, the variance component  $\Sigma_{jj}$  is not identifiable from marginal success probabilities. We impose  $\Sigma_{jj} = 1$ , which is standard and resolves this non-identifiability. For our proposed Algorithm 1, we post-process MCMC samples  $\Sigma_{ij}^{*l} = \Sigma_{ij}^l / \sqrt{\Sigma_{jj}^l}$ ,  $l = 1, \dots, L$ , where  $L$  is the number of MCMC samples and use  $\Sigma_{ij}^{*l}$  for prediction. We next prove the identifiability of the spatial latent process  $\mathbf{W}$ , which eventually concludes the identifiability conditions for the model parameters in the next theorem.

**Lemma 3.** *For any fixed  $\mathbf{s}$ , let  $Y_j(\mathbf{s}) \mid W_j(\mathbf{s}) \stackrel{\text{ind}}{\sim} \text{EF}(Y_j(\mathbf{s}) \mid W_j(\mathbf{s}), \psi_j)$ ,  $j = 1, \dots, q$ . Define  $b'_j(w) = db_j(w)/dw$  to be the derivative of cumulant function at  $w$  and the mean-value parameter as*

$$\mu_j(\mathbf{s}_i) = E[Y_j(\mathbf{s}_i) \mid W_j(\mathbf{s}_i)] = b'_j(W_j(\mathbf{s}_i)). \quad (12)$$

*Under our model assumption on strict convexity of  $b_j(\cdot)$ , the mapping  $W_j(\mathbf{s}) \mapsto \mu_j(\mathbf{s})$  is one-to-one, ensuring that the canonical parameterization of (4) is uniquely identifiable.*

*Proof.* To establish identifiability, we must show that at a fix location  $\mathbf{s} \in \mathcal{D}$ ,  $W_j(\mathbf{s}) \mapsto \mu_j(\mathbf{s})$  is injective, i.e., for any two values  $W_j(\mathbf{s})$  and  $\widetilde{W}_j(\mathbf{s})$ , the equation

$$b'_j(W_j(\mathbf{s})) = b'_j(\widetilde{W}_j(\mathbf{s})) \implies W_j(\mathbf{s}) = \widetilde{W}_j(\mathbf{s}).$$

Since  $b_j$  is strictly convex by assumption, its derivative  $b'_j$  is strictly increasing, which guarantees that  $b'_j$  is injective. Thus, the mapping  $W_j(\mathbf{s}) \mapsto \mu_j(\mathbf{s})$  is injective. Given that the

injectivity is sufficient for identifiability, the canonical parameterization is identifiable.  $\square$

Lemma 3 ensures that the latent process matrix of our model is identifiable. In spite of having identifiability of  $\mathbf{W}$ , the consistent estimability cannot be guaranteed due to non-replicated spatial data. This is a major challenge which directly influences the quality of estimation of  $\mathbf{W}$ , consequently, the model parameters. Since the model parameters are hierarchically dependent on  $\mathbf{W}$  from the second layer in the Figure 1, the consequences of bad estimation of  $\mathbf{W}$  are followed to the next layer as well. We now present a result that provides conditions for the identifiability of the model parameters  $\mathbf{B}, \Sigma, \phi$ , which directly impact inference.

**Theorem 4.** *If the covariate matrix  $\mathbf{X}$  over  $n$ -locations has full column rank  $p < n$ , the regression coefficient matrix  $\mathbf{B}$  in our model (8) is identifiable. If  $\nu$  is known, then  $\Sigma$  is identifiable up to a multiplicative constant and  $\Sigma/\phi^{2\nu}$  is identifiable.*

*Proof.* We define  $\boldsymbol{\theta} = [\text{vec}(\mathbf{B})^\top, \text{vec}(\Sigma)^\top, \phi]^\top$  to be the vector of finite-dimensional parameters in (8). Then the likelihood of  $\boldsymbol{\theta}$ , conditioning on the latent random matrix  $\mathbf{W}$ , is given by

$$L(\boldsymbol{\theta}|\mathbf{W}) = \frac{1}{\sqrt{(2\pi)^{nq} |\Sigma|^{2n} |\mathbf{K}_\phi|^{2q}}} \exp \left\{ -\frac{1}{2} \text{tr} \left( \Sigma^{-1} (\mathbf{W} - \mathbf{X}\mathbf{B})^\top \mathbf{K}_\phi^{-1} (\mathbf{W} - \mathbf{X}\mathbf{B}) \right) \right\}.$$

We denote twice the negative log-likelihood  $-2 \log L(\boldsymbol{\theta}|\mathbf{W})$  as

$$l(\boldsymbol{\theta}|\mathbf{W}) = n \log |\Sigma| + q \log |\mathbf{K}_\phi| + \text{tr} \left( \Sigma^{-1} (\mathbf{W} - \mathbf{X}\mathbf{B})^\top \mathbf{K}_\phi^{-1} (\mathbf{W} - \mathbf{X}\mathbf{B}) \right). \quad (13)$$

We first show the identifiability of the regression coefficient matrix  $\mathbf{B}$ . Suppose we consider two arbitrary vectors of parameters  $\boldsymbol{\theta}_1 = [\text{vec}(\mathbf{B}_1)^\top, \text{vec}(\Sigma_1)^\top, \phi_1]^\top$  and  $\boldsymbol{\theta}_2 = [\text{vec}(\mathbf{B}_2)^\top, \text{vec}(\Sigma_2)^\top, \phi_2]^\top$ . We must show that if  $\boldsymbol{\theta}_1 \neq \boldsymbol{\theta}_2$ , then  $l(\boldsymbol{\theta}_1|\mathbf{W})$  and  $l(\boldsymbol{\theta}_2|\mathbf{W})$  are different on a set of  $\mathbf{W}$  with positive Lebesgue measure. Since the Matrix-Normal distribution of  $\mathbf{W}$  is characterized by its mean matrix  $\mathbf{X}\mathbf{B}$  and Kronecker-product derived covariance matrix  $\boldsymbol{\Omega}_\phi$  uniquely, it suffices to show that  $\boldsymbol{\theta}_1 \neq \boldsymbol{\theta}_2$  implies either different means or different covariance matrices. Suppose  $\mathbf{B}_1$  and  $\mathbf{B}_2$  are two distinct values of  $\mathbf{B}$  which corresponds to distinct  $\boldsymbol{\theta}_1$  and  $\boldsymbol{\theta}_2$ . Since  $\mathbf{X}$  has full column rank, then  $\mathbf{X}\mathbf{B}_1 \neq \mathbf{X}\mathbf{B}_2$ . Consequently,  $l(\boldsymbol{\theta}_1|\mathbf{W}) \neq l(\boldsymbol{\theta}_2|\mathbf{W})$ . The mapping of  $\mathbf{B} \rightarrow l(\boldsymbol{\theta}|\mathbf{W})$  is thus injective, and we have already shown  $\mathbf{W}$  is identifiable in Lemma 3. Hence, the regression coefficient matrix  $\mathbf{B}$  is identifiable in our model.

Now we derive the conditions of identifiability of  $\Sigma$  and  $\phi$ . Since the random matrix  $\mathbf{W}$  is Matrix-Normal with covariance parameters  $\mathbf{K}_\phi$  and  $\Sigma$  is equivalent to assuming that  $\text{vec}(\mathbf{W})$  is multivariate normal with covariance  $\Sigma \otimes \mathbf{K}_\phi$  (follows from (9)). We interpret  $\mathbf{K}_\phi$  as the common covariance matrix of the columns of  $\mathbf{W}$  and  $\Sigma$  as the common covariance matrix of the rows of  $\mathbf{W}$ . Indeed, for any  $c > 0$ ,  $(c^{-1}\Sigma) \otimes (c\mathbf{K}_\phi) = \Sigma \otimes \mathbf{K}_\phi$ . However, without further restrictions, this interpretation is problematic since  $\mathbf{K}_\phi$  and  $\Sigma$  are only identified up to scaling by a constant. The identifiability of the microergodic parameter  $\Sigma/\phi^{2\nu}$  is a direct corollary of Theorem 3 of [Bachoc et al. \(2022\)](#).  $\square$

As discussed by [Zhang \(2004\)](#), the estimability of weakly identified parameters is not possible in multivariate geostatistics under infill asymptotics, where the number of locations increases in a restricted compact domain. However, according to [Stein \(1999\)](#), we obtain asymptotically equivalent predictions from a model with such inconsistently estimated parameters. Moreover, if  $\mathbf{K}_\phi$  and  $\Sigma$  are unidentified, one usually has to focus on estimation and interpretation only on their Kronecker product  $\Sigma \otimes \mathbf{K}_\phi$ . For fitting purposes, an identifiability constraint such as  $\|\Sigma\| = 1$  (unit spectral norm) or  $\mathbf{K}_\phi^{(1,1)} = 1$  (unit leading entry) is often imposed in the literature. Here, the spatial correlation matrix  $\mathbf{K}_\phi$  is indeed with  $\mathbf{K}_\phi^{(i,i)} = 1$  for all  $i = 1, \dots, n$ , hence we do not require any identifiability constraint unless we have a logit link for  $j$ -th response. The following subsection discusses a scalable approach we adopt for large spatial datasets.

## 2.4 Extension to high-dimensions: Vecchia approximation

A major drawback of GP-based methods is that inference time typically grows cubically in the size of the training set due to the necessity of inverting a dense covariance matrix, making them impractical for large spatial datasets. To enable scalable inference, we adopt the Vecchia approximation ([Vecchia, 1988](#)), which approximates the joint distribution of the latent process  $\mathbf{W}$  by factorizing it into conditionals that depend only on a small subset of ordered locations. Let  $\mathcal{N}(i) = \{i+1, \dots, n\}$  be the set of “succeeding” ordered indices for the  $i$ th ordered location, which is the “full” conditioning set. We induce sparsity into the spatial random effect  $\mathbf{W}$  by defining a reduced conditioning index set  $\mathcal{M}(i) \subset \mathcal{N}(i)$  for the  $i$ -th ordered location. Here, we restrict  $\mathcal{M}(i)$  to be a set of size at most  $m$  for the  $i$ th location. The latent process thus at the  $i$ -th ordered location is conditionally dependent only on the succeeding indices that are contained in  $\mathcal{M}(i)$  of size less than or equal to  $m$ .

We denote the corresponding latent process as

$$\mathcal{W}_{\mathcal{M}(i)} = \{\mathcal{W}(\mathbf{s}_j) : j \in \mathcal{M}(i)\}.$$

The Vecchia approximation to the joint density of  $\mathbf{W}$  with sparsity parameter  $m$  is given by

$$\tilde{\pi}_m(\mathbf{W} \mid \boldsymbol{\theta}) = \prod_{i=1}^n \pi(\mathcal{W}(\mathbf{s}_i) \mid \mathcal{W}_{\mathcal{M}(i)}, \boldsymbol{\theta}). \quad (14)$$

As the number of nearest neighbours  $m$  increases,  $\tilde{\pi}_m(\mathbf{W} \mid \boldsymbol{\theta})$  becomes a better approximation to the true joint density, and is exact when  $m = n-1$ . [Schafer et al. \(2021\)](#) discuss a detailed theoretical analysis of the Kullback-Leibler loss of the Vecchia approximated density with sparsity parameter  $m$ . In practice, a small  $m$  achieves a favorable balance between accuracy and computational cost. We use the max-min ordering of spatial locations ([Guinness, 2018](#)) with nearest-neighbor conditioning, so that each  $\mathcal{M}(i)$  consists of the  $\min\{m, n+1-i\}$  closest succeeding ordered locations. In particular, letting  $(\mathbf{K}_{\phi,(m)})^{-1}$  be the Vecchia approximated spatial precision matrix of  $\mathbf{W}$  based on  $m$  nearest neighbours ( $m$ -NN) and  $\mathbf{U}_{\phi,(m)}$  be its sparse upper-triangular Cholesky factor, we modify the Matrix-Normal distribution of latent Gaussian matrix  $\mathbf{W}$  from (9) as

$$\mathbf{W} \sim \mathcal{MN}_{n,q}(\mathbf{X}\mathbf{B}, \mathbf{K}_{\phi,(m)}) = (\mathbf{U}_{\phi,(m)}^\top \mathbf{U}_{\phi,(m)})^{-1}, \boldsymbol{\Sigma}). \quad (15)$$

It is possible to compute each of the  $n$  rows of  $\mathbf{U}$  in  $\mathcal{O}(m^3)$  time in parallel. However, we implement it in a single core with a reduced computational cost of inverting the Vecchia approximated spatial covariance matrix  $\mathbf{K}_{\phi,(m)}$  of  $\mathcal{O}(nm^3)$  when  $m \ll \sqrt{n}$ .

### 3 Bayesian computation

The number of unknown parameters and latent variables in our model (8), i.e, the dimension of  $(\mathbf{W}, \mathbf{B}, \boldsymbol{\Sigma}, \phi)$  grows as  $\mathcal{O}(nq^2)$  as the number of locations  $n$  and the number of responses  $q$  increase. Jointly updating these many model parameters and the latent spatial effect is cumbersome in high dimensions ([Christensen and Sköld, 2006](#)). We implement a sparsity-informed component-wise sampler to update the unknown parameters, thereby improving the scalability of our algorithm for large spatial datasets. We propose a Matrix-Normal Inverse-Wishart (MNIW) blocked-Gibbs sampler to update  $(\boldsymbol{\Sigma}, \mathbf{B})$  jointly from the posterior

as follows

$$\Sigma \mid \mathbf{W}, \phi \sim \mathcal{IW}_q(\tilde{\mathbf{S}} = \mathbf{S} + \mathbf{W}^\top \mathbf{K}_{\phi, (m)}^{-1} \mathbf{W} + \mathbf{M}^\top \mathbf{V}^{-1} \mathbf{M} - \tilde{\mathbf{M}}^\top \tilde{\mathbf{V}}^{-1} \tilde{\mathbf{M}}, \tilde{v} = v + n),$$

$$\mathbf{B} \mid \Sigma, \phi, \mathbf{W} \sim \mathcal{MN}_{p,q}(\tilde{\mathbf{M}}, \tilde{\mathbf{V}}, \Sigma),$$

where  $\tilde{\mathbf{V}} = (\mathbf{X}^\top \mathbf{K}_{\phi, (m)}^{-1} \mathbf{X} + \mathbf{V}^{-1})^{-1}$ ,  $\tilde{\mathbf{M}} = \tilde{\mathbf{V}}(\mathbf{X}^\top \mathbf{K}_{\phi, (m)}^{-1} \mathbf{W} + \mathbf{V}^{-1} \mathbf{M})$ . The derivations are given in Appendix B. We update  $\phi$  using a truncated normal random-walk proposal centered at the current value in the domain  $(0, b_\phi)$ . Updating the spatial random effects  $\mathbf{W} \in \mathbb{R}^{n \times q}$  via random-walk Metropolis–Hastings is computationally challenging due to strong posterior correlations and the spatial cross-covariance structure. These lead to poor mixing, high autocorrelation, and low acceptance rates, which is consistent with observations in Rue and Martino (2007). Moreover, proposal tuning is complex due to scale heterogeneity across components of  $\mathbf{W}$ . While samplers like preconditioned Crank–Nicolson (Cotter et al., 2013; Rudolf and Sprungk, 2022) can exploit the posterior geometry of  $\mathbf{W}_{n \times q}$  in our model, they require  $nq$  tuning parameters. We employ elliptical slice sampling (Murray et al., 2010), which is well-suited for models with latent Gaussian priors. Elliptical slice sampling is tuning-free, requires no gradients, MAP estimates, or Hessian approximations, and is scalable to high-dimensional settings when used with the Vecchia accelerated sampling from the Gaussian proposal in high dimensions. In our case, given  $\mathbf{B}, \Sigma, \phi, \mathbf{Y}$ , the Gaussian prior in the full-conditional posterior of  $\mathbf{W}$  ensures compatibility with elliptical slice sampling, making it a robust and efficient choice. In Step 2 of Table 1, we update the model parameters  $(\mathbf{W}, \mathbf{B}, \Sigma, \phi)$  in a sequential ordering based on the dimension of the component. We first update  $\phi$ , then update  $(\Sigma, \mathbf{B})$  jointly, and lastly  $\mathbf{W}$ . We recommend a warm start for initializing the parameters, so that the chain quickly explores the high-probability region. We refer to Appendix C for the detailed steps of the elliptical slice sampling algorithm for updating  $\mathbf{W}$ .

## 4 Predictive modeling

An important objective of spatial models is to predict responses at unobserved locations  $\mathcal{U} = \{s_1^*, s_2^*, \dots, s_u^*\}$  distinct from  $\mathcal{S}$ , in the presence of covariates. Let us denote the stacked matrices for responses, latent process, and covariates over the unobserved locations

$\mathcal{U}$ , respectively, as

$$\mathbf{Y}^* = \begin{bmatrix} \mathcal{Y}(\mathbf{s}_1^*)^\top \\ \mathcal{Y}(\mathbf{s}_2^*)^\top \\ \vdots \\ \mathcal{Y}(\mathbf{s}_u^*)^\top \end{bmatrix}_{u \times q}, \quad \mathbf{W}^* = \begin{bmatrix} \mathcal{W}(\mathbf{s}_1^*)^\top \\ \mathcal{W}(\mathbf{s}_2^*)^\top \\ \vdots \\ \mathcal{W}(\mathbf{s}_u^*)^\top \end{bmatrix}_{u \times q}, \quad \text{and} \quad \mathbf{X}^* = \begin{bmatrix} \mathcal{X}(\mathbf{s}_1^*)^\top \\ \mathcal{X}(\mathbf{s}_2^*)^\top \\ \vdots \\ \mathcal{X}(\mathbf{s}_u^*)^\top \end{bmatrix}_{u \times p}.$$

The goal in predictive modeling is to compute the posterior predictive distribution (PPD) of  $\mathbf{Y}^*$  given the observed data matrix  $\mathbf{Y}$ . We denote the PPD as

$$\pi(\mathbf{y}^* | \mathbf{y}) = \int \int \pi(\mathbf{y}^* | \mathbf{w}^*) \pi(\mathbf{w}^* | \mathbf{w}) \pi(\mathbf{w} | \boldsymbol{\theta}) \pi(\boldsymbol{\theta} | \mathbf{y}) d\mathbf{w}^* d\mathbf{w} d\boldsymbol{\theta}, \quad (16)$$

where  $\boldsymbol{\theta} = (\mathbf{B}, \boldsymbol{\Sigma}, \phi)^\top$  represents the model parameters. Given our model assumptions, the joint distribution of  $[\mathbf{W}^{*\top}, \mathbf{W}^\top]^\top$  for locations in  $\mathcal{U} \cup \mathcal{S}$  is

$$\begin{bmatrix} \mathbf{W}^* \\ \mathbf{W} \end{bmatrix} \sim \mathcal{MN}_{u+n, q} \left( \begin{bmatrix} \mathbf{X}^* \mathbf{B} \\ \mathbf{X} \mathbf{B} \end{bmatrix}, \mathbf{K}_{\phi, (m)}^{(u+n)} = \begin{bmatrix} \mathbf{K}_{\phi, (m)}^{(u, u)} & \mathbf{K}_{\phi, (m)}^{(u, n)} \\ \mathbf{K}_{\phi, (m)}^{(n, u)} & \mathbf{K}_{\phi, (m)}^{(n, n)} \end{bmatrix}, \boldsymbol{\Sigma} \right).$$

For our proposed model, denoting  $\mathbf{M}_{W*} = \mathbf{X}^* \mathbf{B} + \mathbf{K}_{\phi, (m)}^{(u, n)} (\mathbf{K}_{\phi, (m)}^{(n, n)})^{-1} (\mathbf{W} - \mathbf{X} \mathbf{B})$  and  $\mathbf{K}_{W*} = \mathbf{K}_{\phi, (m)}^{(u, u)} - \mathbf{K}_{\phi, (m)}^{(u, n)} (\mathbf{K}_{\phi, (m)}^{(n, n)})^{-1} \mathbf{K}_{\phi, (m)}^{(n, u)}$ , the joint Gaussian distribution of  $[\mathbf{W}^{*\top}, \mathbf{W}^\top]^\top$  leads to the following conditional distribution of latent process

$$\mathbf{W}^* | \mathbf{W}, \mathbf{B}, \boldsymbol{\Sigma}, \phi \sim \mathcal{MN}_{u, q} (\mathbf{M}_{W*}, \mathbf{K}_{W*}, \boldsymbol{\Sigma}). \quad (17)$$

However, computing the covariance blocks obtained from the locations of  $\mathcal{U} \cup \mathcal{S}$  in high dimensions (i.e., large  $n$  and  $u$ ) becomes computationally challenging, as the covariance structure must be evaluated repeatedly within posterior sampling or prediction. Here, the Vecchia approximation (14) avoids dense matrix computations by operating directly on the joint precision matrix  $\mathbf{Q}_{\phi, (m)}^{(u+n)} = (\mathbf{K}_{\phi, (m)}^{(u+n)})^{-1}$  corresponding to the latent process. Denoting the joint precision matrix partitioned conformably as

$$\mathbf{Q}_{\phi, (m)}^{(u+n)} = \begin{bmatrix} \mathbf{Q}_{\phi, (m)}^{(u, u)} & \mathbf{Q}_{\phi, (m)}^{(u, n)} \\ \mathbf{Q}_{\phi, (m)}^{(n, u)} & \mathbf{Q}_{\phi, (m)}^{(n, n)} \end{bmatrix}. \quad (18)$$

Instead of sampling with joint covariance matrix  $\mathbf{K}_{\phi, (m)}^{(u+n)}$ , we reparameterize (17) as

$$\mathbf{W}^* \mid \mathbf{W}, \mathbf{B}, \Sigma, \phi \sim \mathcal{MN}_{u,q} \left( \mathbf{X}^* \mathbf{B} - (\mathbf{Q}_{\phi, (m)}^{(u,u)})^{-1} \mathbf{Q}_{\phi, (m)}^{(u,n)} (\mathbf{W} - \mathbf{X} \mathbf{B}), (\mathbf{Q}_{\phi, (m)}^{(u,u)})^{-1}, \Sigma \right), \quad (19)$$

and draw samples from posterior predictive process using a Vecchia approximated sparse Cholesky factorization of  $\mathbf{Q}_{\phi, (m)}^{(u+n)}$ . This form enables efficient sampling and inference by utilizing only the sparse structure, without the need to invert the full covariance matrix explicitly. We use Monte Carlo integration in (16) to generate posterior samples from the distribution of  $\mathbf{Y}^* | \mathbf{Y}$ . Our scalable approach ensures both tractability and accuracy in high-dimensional spatial prediction, particularly for mixed-type responses where standard Gaussian assumptions are not applicable.

The overall computational complexity presented in Table 1 is broken down across three primary stages. In Step 1, we carry out pre-computing foundations for Vecchia approximation on the training set  $\mathcal{S}$  and the test set  $\mathcal{U}$ . We perform fast max-min ordering as suggested in [Guinness \(2018\)](#) with leading computational costs of  $\mathcal{O}(n^{*2} \log n^*)$  where  $n^* = n+u$ . We store the distance matrices computed on  $\mathcal{U}$  and  $\mathcal{S}$  for repeated use in MCMC iterations. In Step 2, we perform posterior sampling using the MCMC algorithm described in Section 3, where the dominant per iteration costs to update  $\phi$  and  $\mathbf{W}$  significantly decrease to order of  $\mathcal{O}(nm^3)$  where a small  $m$  provides good approximation, instead of using a full GP with order  $\mathcal{O}(n^3)$ . We also constrain  $\Sigma_{jj} = 1$  when the  $j$ -th response is Binomial during post-processing of MCMC samples. In Step 3, we generate predictive samples at a set of new spatial locations  $\mathcal{U}$  where all the responses are unknown, with a reduced computational cost of  $\mathcal{O}(um^3)$ . Unlike standard GP models that require  $\mathcal{O}(u^3)$  operations for dense covariance matrix factorizations, our algorithm achieves linear scaling in the number of locations  $n$  due to the use of a fixed number of local conditioning sets of size  $m \ll n$ , ensuring practical scalability even in high-dimensional spatial domains.

## 5 Data analysis

We evaluate the statistical performance of our proposed joint Bayesian model for mixed-type spatial responses by comparing it with a commonly used alternative of separate modeling. By separate modeling, we refer to the conventional approach where each response is treated independently, despite the possibility of cross-response dependence in the true data-generating process (i.e.,  $\Sigma_{ij} \neq 0$  for  $i \neq j$ ). These models inherently assume  $\Sigma_{ij} = 0$  and fit independent univariate latent GP, each with its own mean structure and covariance

**Table 1:** Posterior inference and prediction for mixed-type response model

Steps	Description	Flops
1	<b>Pre-computing steps for Vecchia approximation</b> <b>Require:</b> family of length $q$ , $\mathcal{S}$ , $\mathcal{U}$ of size $n$ and $u$ . Denote $n^* = n + u$ and obtain $\max\text{-}\min(\mathcal{S})$ and $\max\text{-}\min(\mathcal{U} \cup \mathcal{S})$ . Construct $\text{NN}_{\mathcal{S}} = \{\mathcal{M}(i) : \mathbf{s}_i \in \mathcal{S}\}$ and $\text{NN}_{\mathcal{U} \cup \mathcal{S}} = \{\mathcal{M}(i) : \mathbf{s}_i \in \mathcal{U} \cup \mathcal{S}\}$ . Store $D_{\mathcal{S}} = \{\ \mathbf{s}_i - \mathbf{s}_j\ _2 : i, j \in \text{NN}_{\mathcal{S}}\}$ , $D_{\mathcal{U} \cup \mathcal{S}} = \{\ \mathbf{s}_i - \mathbf{s}_j\ _2 : i, j \in \text{NN}_{\mathcal{U} \cup \mathcal{S}}\}$ .	$\mathcal{O}(n^{*2} \log n^*)$
2	<b>MCMC algorithm for posterior inference on <math>\mathcal{S}</math></b> <b>For</b> $l = 1, \dots, L$ : sample posterior parameters. Construct $\mathbf{U}_{\phi, (m)} = \text{chol}(\mathbf{K}_{\phi, (m)}^{-1})$ as described in (15). Construct $\mathbf{U}_{\mathbf{V}} = \text{chol}(\mathbf{V}^{-1})$ . Compute $\mathbf{U}_{\phi, (m)} \mathbf{X}$ and $\mathbf{U}_{\phi, (m)} \mathbf{W}$ . Obtain $\tilde{\mathbf{V}}$ , $\tilde{\mathbf{M}}$ , $\tilde{\mathbf{S}}$ , $\tilde{v}$ : $\tilde{\mathbf{V}} = ((\mathbf{U}_{\phi, (m)} \mathbf{X})^\top (\mathbf{U}_{\phi, (m)} \mathbf{X}) + \mathbf{U}_{\mathbf{V}}^\top \mathbf{U}_{\mathbf{V}})^{-1}$ and compute $\mathbf{U}_{\tilde{\mathbf{V}}} = \text{chol}(\tilde{\mathbf{V}})$ . $\tilde{\mathbf{M}} = \tilde{\mathbf{V}} ((\mathbf{U}_{\phi, (m)} \mathbf{X})^\top (\mathbf{U}_{\phi, (m)} \mathbf{W}) + \mathbf{U}_{\mathbf{V}}^\top \mathbf{U}_{\mathbf{V}} \mathbf{M})$ . $\tilde{\mathbf{S}} = \mathbf{S} + (\mathbf{U}_{\phi, (m)} \mathbf{W})^\top (\mathbf{U}_{\phi, (m)} \mathbf{W}) + (\mathbf{U}_{\mathbf{V}} \mathbf{M})^\top (\mathbf{U}_{\mathbf{V}} \mathbf{M}) - (\mathbf{U}_{\tilde{\mathbf{V}}} \tilde{\mathbf{M}})^\top (\mathbf{U}_{\tilde{\mathbf{V}}} \tilde{\mathbf{M}})$ . $\tilde{v} = v + n$ . Sample $\phi^{(l)}$ via Metropolis-Hastings with truncated-normal proposal. Sample $\Sigma^{(l)} \sim \mathcal{IW}(\tilde{\mathbf{S}}, \tilde{v})$ and find $\mathbf{U}_{\Sigma^{(l)}} = \text{chol}(\Sigma^{(l)})$ . Sample $\mathbf{B}^{(l)} \sim \mathcal{MN}_{p, q}(\tilde{\mathbf{M}}, \tilde{\mathbf{V}}, \Sigma^{(l)})$ : Sample $\mathbf{Z} \sim \mathcal{MN}_{p, q}(0, \mathbf{I}_p, \mathbf{I}_q)$ . Generate $\mathbf{B}^{(l)} = \tilde{\mathbf{M}} + \mathbf{U}_{\tilde{\mathbf{V}}} \mathbf{Z} \mathbf{U}_{\Sigma^{(l)}}^\top$ as in Appendix C. Sample $\mathbf{W}^{(l)}$ via elliptical slice sampling as in Algorithm 1. <b>For</b> $j = 1, \dots, q$ : <b>If</b> family[j] = "Binomial" : $\Sigma_{jj}^{(l)} = 1$ and $\Sigma_{ij}^{(l)} = \Sigma_{ij}^{(l)} / \sqrt{\Sigma_{jj}^{(l)}}$ <b>End</b> Save $\{(\mathbf{W}^{(l)}, \mathbf{B}^{(l)}, \Sigma^{(l)}, \phi^{(l)}) : l = 1, \dots, L\}$	$\mathcal{O}(nm^3)$ $\mathcal{O}(p^3)$ $\mathcal{O}(nm(p + q))$ $\mathcal{O}(p^3)$ $\mathcal{O}(npq)$ $\mathcal{O}(nq^2)$ $\mathcal{O}(1)$ $\mathcal{O}(nm^3)$ $\mathcal{O}(q^3)$ $\mathcal{O}(pq)$ $\mathcal{O}(pq^2 + q^2)$ $\mathcal{O}(nm^3)$
3	<b>Vecchia-based prediction on <math>\mathcal{U}</math></b> Construct $\tilde{\mathbf{D}} = (\mathbf{Q}_{\phi, (m)}^{(u, u)})^{-1}$ , $\mathbf{U}_{\tilde{\mathbf{D}}} = \text{chol}(\tilde{\mathbf{D}})$ and $\tilde{\mathbf{A}}_{\phi, (m)} = \tilde{\mathbf{D}} \mathbf{Q}_{\phi, (m)}^{(u, n)}$ . Sample $\mathbf{W}^{*(l)} \sim \mathcal{MN}_{u, q}(\mathbf{X}^* \mathbf{B}^{(l)} - \tilde{\mathbf{A}}(\mathbf{W} - \mathbf{X} \mathbf{B}^{(l)}), \tilde{\mathbf{D}}, \Sigma^{(l)})$ : Sample $\mathbf{Z} \sim \mathcal{MN}_{u, q}(0, \mathbf{I}_u, \mathbf{I}_q)$ . Generate $\mathbf{W}^{*(l)} = \mathbf{X}^* \mathbf{B}^{(l)} - \tilde{\mathbf{A}}(\mathbf{W} - \mathbf{X} \mathbf{B}^{(l)}) + \mathbf{U}_{\tilde{\mathbf{D}}} \mathbf{Z} \mathbf{U}_{\Sigma^{(l)}}^\top$ . Generate $Y_j(\mathbf{s}_i^*) \mid W_j(\mathbf{s}_i^*) \sim \text{EF}(W_j(\mathbf{s}_i^*), \psi_j)$ , $\mathbf{s}_i^* \in \mathcal{U}$ . Save $\{\mathbf{Y}^{*(l)} : l = 1, \dots, L\}$ .	$\mathcal{O}(um^3)$ $\mathcal{O}(uq)$ $\mathcal{O}(n(q^2 + u)q)$ $\mathcal{O}(u)$

kernel to account for spatial dependence, thereby ignoring potential dependence between different response types.

We use weak prior information for the regression coefficient matrix  $\mathbf{B}$  by specifying the mean matrix of  $\mathbf{B}$  as  $\mathbf{M} = \mathbf{0}$  and the covariance matrix  $\mathbf{V} = 100\mathbf{I}_p$ . For the cross-response covariance  $\Sigma$ , we choose  $\mathbf{S} = \mathbf{I}_q$  and  $v = q + 1$ , providing a weakly-informative prior. The full conditional posterior of  $\Sigma$  admits a valid density and thus the posterior is proper. We recommend a reasonable choice for the smoothness parameter  $\nu$  in the Matérn kernel obtained by the empirical semivariogram from exploratory data analysis, with smoother curves indicating larger  $\nu$ . The choice of  $\nu = 0.5$  simplifies the kernel (7) to an exponential kernel, while the choice of  $\nu = \infty$  gives the squared-exponential kernel. The hyperparameter  $b_\phi$  for the spatial range parameter,  $\phi$ , is chosen so that the effective range corresponds to a correlation of 0.05 at the domain diameter  $\Delta = \max_{i,j} \|\mathbf{s}_i - \mathbf{s}_j\|_2$ . We evaluate the predictive performance of our proposed model over a separate model by computing Watanabe–Akaike Information Criterion (WAIC) over the full dataset and the Expected Log-Pointwise Density (ELPD) at the hold-out locations, which are the benchmark criteria as suggested by [Cooper et al. \(2025\)](#). The lower values of WAIC and larger values of ELPD are indicators of a better model selection rule. The R codes to reproduce the simulation studies and real data analysis are available on GitHub<sup>1</sup>.

## 5.1 Simulation studies

Our analysis is based on studying the quality of estimation and the model performance in terms of the strength of prediction. We consider two different case studies based on “Gaussian-Poisson” and “Gaussian-Bernoulli” response spatial data in both small-dimensional ( $n = 100$ ) and high-dimensional ( $n = 2500$ ) setups on a unit square  $\mathcal{D} = [0, 1]^2$ . We leave out 20% of the randomly chosen locations for predictive analysis. For each of the following cases, we segment our analysis further on weak and strong spatial correlation  $\phi_0 \in \{0.1, 0.5\}$  and dependent and independent cross-correlation  $\Sigma^{(0)} \in \{[(2, 1)^\top, (1, 1)^\top], \text{diag}(2, 1)\}$ . At any location  $\mathbf{s}$ , we consider the linear covariates as  $\mathcal{X}(\mathbf{s}) = [1, \text{lon}(\mathbf{s}), \text{lat}(\mathbf{s})]^\top$ , which is a standard choice in spatial data analysis and consequently we specify the true regression coefficient matrix as  $\mathbf{B}^{(0)} = [(1.0, -0.5)^\top, (3, 1.5)^\top, (-1.2, 0)^\top]$ .

We run Algorithm 1 corresponding to the model and evaluate the predictive performance and model fit, over 50 replicated datasets. We first highlight the results obtained from the posterior inference of the cross-covariance of two different responses  $\Sigma_{12}$ , which is an

---

<sup>1</sup>Available at [https://github.com/ArghyaStat/Bayesian\\_mixed\\_type\\_spatial\\_model](https://github.com/ArghyaStat/Bayesian_mixed_type_spatial_model)

**Table 2:** Posterior estimation summary of  $\Sigma_{12}$  (posterior mean, 95% posterior credible interval, and coverage probability) across 50 replicated datasets under varying spatial correlation ( $\phi_0$ , the true value of  $\phi$ ) and varying cross-covariance matrix ( $\Sigma^{(0)}$ , the true value of  $\Sigma$ ) for Gaussian-Poisson responses.

$\text{vec}(\Sigma^{(0)})$	$\phi_0$	Posterior mean (SE)	Credible interval (SE)	Coverage (SE)
Sample size: $n = 100$				
$[2, 1, 1, 1]^\top$	0.5	0.357 (0.037)	[-0.478 (0.052), 1.117 (0.042)]	0.62 (0.069)
	0.1	0.857 (0.057)	[-0.168 (0.088), 1.778 (0.056)]	1.00 (0.000)
Sample size: $n = 2500$				
$[2, 1, 1, 1]^\top$	0.5	0.737 (0.019)	[0.528 (0.018), 1.021 (0.019)]	0.60 (0.070)
	0.1	0.932 (0.011)	[0.775 (0.010), 1.140 (0.016)]	0.94 (0.034)
Sample size: $n = 100$				
$[2, 0, 0, 1]^\top$	0.5	0.036 (0.036)	[-0.801 (0.044), 0.869 (0.044)]	1.00 (0.000)
	0.1	0.016 (0.074)	[-1.174 (0.078), 1.172 (0.077)]	0.94 (0.034)
Sample size: $n = 2500$				
$[2, 0, 0, 1]^\top$	0.5	-0.008 (0.015)	[-0.168 (0.019), 0.163 (0.017)]	0.88 (0.046)
	0.1	-0.009 (0.015)	[-0.168 (0.017), 0.149 (0.017)]	0.86 (0.050)

important parameter for our model. In Table 2, we observe that for Scenario-1, the posterior credible interval does not contain zero, and the average posterior mean across 50 replicated datasets is also significantly higher than zero. Consequently, joint modeling is essential in this case. Whereas, Table 2 also suggests that when the bivariate GP is modeled with  $\Sigma_{12} = 0$ , the posterior mean is well estimated and the credible interval contains the true value. For small sample data analysis of Gaussian-Bernoulli responses in Table 3, we observe that zero is contained in Scenario 1 due to the challenging estimation of the parameter in the presence of non-identifiability and a small sample size. We observe positive results in a high-dimensional case study and claim that our joint model captures the cross-dependence, which is completely disregarded in a separate analysis.

Next, we report the predictive performance, along with its respective standard errors. Simulation studies with different response pairs and varying strengths of spatial correlation show that the predictive accuracy of the multivariate model is better than that of the separate model when the model is correctly specified. The separate model does not always provide better predictive inference than the multivariate model, especially when parameters

**Table 3:** Posterior estimation summary of  $\Sigma_{12}$  (posterior mean, 95% posterior credible interval, and coverage probability) across 50 replicated datasets under varying spatial correlation ( $\phi_0$ , the true value of  $\phi$ ) and varying cross-covariance matrix ( $\Sigma^{(0)}$ , the true value of  $\Sigma$ ) for Gaussian-Bernoulli responses.

vec( $\Sigma^{(0)}$ )	$\phi_0$	Posterior mean (SE)	Credible interval (SE)	Coverage (SE)
Sample size: $n = 100$				
$[2, 1, 1, 1]^\top$	0.5	0.357(0.037)	$[-0.478(0.052), 1.117(0.042)]$	0.62(0.069)
	0.1	0.857(0.057)	$[-0.168(0.088), 1.778(0.056)]$	1.00(0.000)
Sample size: $n = 2500$				
$[2, 1, 1, 1]^\top$	0.5	0.737(0.019)	$[0.528(0.018), 1.021(0.019)]$	0.60(0.070)
	0.1	0.932(0.011)	$[0.775(0.010), 1.140(0.016)]$	0.94(0.034)
Sample size: $n = 100$				
$[2, 0, 0, 1]^\top$	0.5	0.036(0.036)	$[-0.801(0.044), 0.869(0.044)]$	1.00(0.000)
	0.1	0.016(0.074)	$[-1.174(0.078), 1.172(0.077)]$	0.94(0.034)
Sample size: $n = 2500$				
$[2, 0, 0, 1]^\top$	0.5	-0.008(0.015)	$[-0.168(0.019), 0.163(0.017)]$	0.88(0.046)
	0.1	-0.009(0.015)	$[-0.168(0.017), 0.149(0.017)]$	0.86(0.050)

**Table 4:** Predictive performance summary for Gaussian–Poisson response under varying spatial correlation ( $\phi_0$ , the true value of  $\phi$ ) and varying cross-covariance matrix ( $\Sigma^{(0)}$ , the true value of  $\Sigma$ ), based on 50 replicated datasets.

vec( $\Sigma^{(0)}$ )	$\phi_0$	Model	WAIC (SE)	ELPD (SE)	Coverage (SE)
Sample size: $n = 100$					
$[2, 1, 1, 1]^\top$	0.5	Joint	<b>536.191 (1.243)</b>	<b>-5.6335 (0.053)</b>	0.9590 (0.001)
		Separate	544.414 (1.253)	-5.6567 (0.054)	0.9555 (0.001)
	0.1	Joint	<b>583.678 (0.679)</b>	-5.7677 (0.028)	0.9620 (0.001)
		Separate	604.722 (0.684)	<b>-5.7647 (0.027)</b>	0.9605 (0.001)
$[2, 0, 0, 1]^\top$	0.5	Joint	529.196 (1.338)	-5.4966 (0.037)	0.9505 (0.001)
		Separate	<b>528.625 (1.329)</b>	<b>-5.4811 (0.037)</b>	0.9535 (0.001)
	0.1	Joint	602.598 (0.585)	-5.5815 (0.021)	0.9490 (0.001)
		Separate	<b>600.513 (0.569)</b>	<b>-5.5667 (0.021)</b>	0.9590 (0.001)
Sample size: $n = 2500$					
$[2, 1, 1, 1]^\top$	0.5	Joint	<b>12186.669 (28.136)</b>	<b>-6.311 (0.051)</b>	0.9659 (0.000)
		Separate	12267.211 (26.241)	-6.458 (0.054)	0.9528 (0.001)
	0.1	Joint	<b>12855.419 (10.260)</b>	<b>-6.9812 (0.022)</b>	0.9640 (0.001)
		Separate	12963.125 (10.681)	-7.296 (0.025)	0.9655 (0.002)
$[2, 0, 0, 1]^\top$	0.5	Joint	12211.795 (27.139)	<b>-6.160 (0.038)</b>	0.9663 (0.000)
		Separate	<b>12151.443 (26.704)</b>	-6.224 (0.039)	0.9662 (0.000)
	0.1	Joint	13120.460 (9.847)	<b>-7.014 (0.023)</b>	0.9649 (0.001)
		Separate	<b>12899.387 (9.387)</b>	-7.241 (0.025)	0.9646 (0.001)

are weakly identified. Specifically, from Table 4 for Gaussian-Poisson simulated data with a sample size of 100, we see that our proposed joint model performs better in terms of WAIC and ELPD when spatial correlation is weak ( $\phi = 0.1$ ). Still, both models perform similarly when spatial correlation is substantial ( $\phi = 0.5$ ). When the sample size is large, the differences between models become clearer according to both comparison criteria. Similar patterns are observed in Gaussian-Bernoulli simulations across small and high dimensions. The results demonstrate that multivariate spatial models offer more reliable predictive performance and parameter estimation than separate models for mixed-type responses.

## 5.2 Real data analysis

Wildfires present significant risks to ecosystems, human life, and infrastructure, with far-reaching social and economic consequences. They are also a substantial source of carbon

**Table 5:** Predictive performance summary for Gaussian–Bernoulli response under varying spatial correlation ( $\phi_0$ , the true value of  $\phi$ ) and varying cross-covariance matrix ( $\Sigma^{(0)}$ , the true value of  $\Sigma$ ), based on 50 replicated datasets.

vec( $\Sigma^{(0)}$ )	$\phi_0$	Model	WAIC (SE)	ELPD (SE)	Coverage (SE)
Sample size: $n = 100$					
$[2, 1, 1, 1]^\top$	0.5	Joint	<b>376.259 (1.535)</b>	<b>-3.6487 (0.173)</b>	0.9675 (0.003)
		Separate	378.306 (1.538)	-3.6623 (0.176)	0.9665 (0.004)
	0.1	Joint	<b>413.724 (0.121)</b>	-3.7526 (0.112)	0.9750 (0.003)
		Separate	419.089 (0.994)	<b>-3.7512 (0.113)</b>	0.9745 (0.004)
$[2, 0, 0, 1]^\top$	0.5	Joint	<b>379.780 (1.264)</b>	<b>-3.6418 (0.174)</b>	0.9670 (0.004)
		Separate	380.282 (1.278)	-3.6450 (0.174)	0.9665 (0.004)
	0.1	Joint	420.531 (0.878)	<b>-3.7493 (0.114)</b>	0.9740 (0.004)
		Separate	<b>420.219 (0.838)</b>	-3.7507 (0.114)	0.9745 (0.004)
Sample size: $n = 2500$					
$[2, 1, 1, 1]^\top$	0.5	Joint	<b>8372.217 (15.943)</b>	<b>-3.9321 (0.139)</b>	0.9744 (0.001)
		Separate	8393.196 (16.316)	-3.9413 (0.140)	0.9742 (0.001)
	0.1	Joint	<b>8939.145 (17.234)</b>	<b>-4.2228 (0.066)</b>	0.9735 (0.001)
		Separate	9014.928 (16.095)	-4.2361 (0.066)	0.9760 (0.001)
$[2, 0, 0, 1]^\top$	0.5	Joint	8403.269 (16.943)	<b>-3.9422 (0.139)</b>	0.9741 (0.001)
		Separate	<b>8399.410 (16.316)</b>	-3.9430 (0.140)	0.9742 (0.001)
	0.1	Joint	9023.170 (17.234)	<b>-4.2330 (0.066)</b>	0.9738 (0.001)
		Separate	<b>9015.339 (16.095)</b>	-4.2376 (0.066)	0.9759 (0.001)

dioxide, playing a notable role in intensifying the global greenhouse effect. In the United States, the area affected by wildfires has increased nearly fourfold over the past 40 years (Iglesias et al., 2022), resulting in a sharp rise in federal spending on fire control efforts. These trends underscore the need for flexible statistical methods to accurately predict extreme wildfire events across space, an essential component of fire management that informs resource allocation, risk mitigation, and recovery planning.

We analyze point-referenced wildfire data comprising aggregated monthly counts of wildfire occurrences and corresponding burnt areas within each cell of a regular grid spanning the mainland United States. The dataset, provided for the Extreme Value Analysis (EVA) 2021 data challenge (Opitz, 2023), includes monthly observations from 3,503 grid cells over the mainland United States at a spatial resolution of  $0.5^\circ \times 0.5^\circ$ . It covers a 23-year period (1993–2015) with data recorded for seven months each year (March through September). Despite the discrete nature of wildfire counts (CNTs), much of the existing literature has relied on transformation-based methods to facilitate joint modeling using a bivariate GP. For instance, Cisneros et al. (2023) modeled  $\log(1 + \text{CNT}(\mathbf{s}))$  combining random forest with bivariate GP. While several alternative approaches, such as multi-stage models, have been developed to accommodate zero inflation (Zhang et al., 2023b), we do not aim to compare our model against those. Nonetheless, we acknowledge that more tailored models may improve both fitting and prediction for this dataset. Our primary inferential goal is to evaluate the performance of our proposed multivariate process model in comparison to two conventional modeling approaches outlined as follows,

- $\mathcal{M}_1$  : Joint Gaussian-Poisson model on original scale:  $(\log(1 + \text{BA}(\mathbf{s})), \text{CNT}(\mathbf{s}))$  with (8),
- $\mathcal{M}_2$  : Separate Gaussian-Poisson model on original scale:  $\log(1 + \text{BA}(\mathbf{s}))$  and  $\text{CNT}(\mathbf{s})$ ,
- $\mathcal{M}_3$  : Joint bivariate GP model on transformed scale:  $(\log(1 + \text{BA}(\mathbf{s})), \log(1 + \text{CNT}(\mathbf{s})))$ .

For illustration, we focus on time index 140, corresponding to September 2012, which aligns well with our model assumptions regarding spatial range and cross-covariance separability. A detailed statistical summary, including the number of fires and acres burned, is provided in the US monthly climate reports<sup>2</sup>, which state that “fire seasons” mostly span from July to September. The displayed spatial maps in Figure 2 demonstrate that with high correlations, the responses are spatially localized and concentrated within the domain. Several meteorological and land cover variables can be potentially used as covariates if they are useful and contribute significantly to our data analysis. However, including them

---

<sup>2</sup>Available at <https://www.ncei.noaa.gov>.

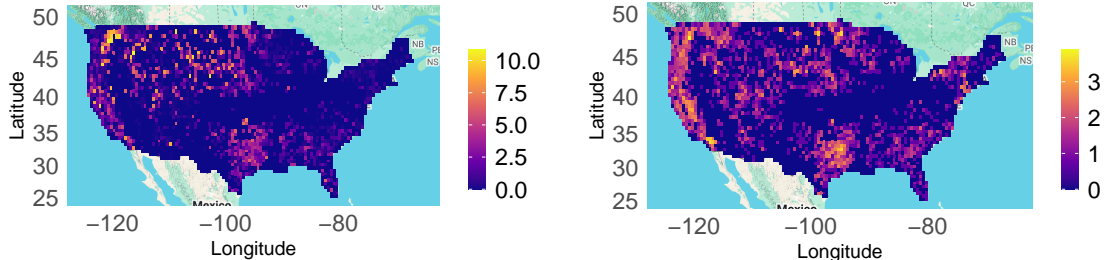


**Figure 2:** Spatial maps of  $\log(1 + \text{BA})$  (left) and  $\log(1 + \text{CNT})$  (right) of September 2012.

in the model can be computationally challenging. We have compared the adjusted- $R^2$  by fitting a simple linear regression model with  $\log(1 + \text{BA}(\mathbf{s}))$  and  $\log(1 + \text{CNT}(\mathbf{s}))$  on the all the covariates and with latitude and longitude as covariates and obtained a mere increase of 0.32 from 0.28 from the later. [Cisneros et al. \(2023\)](#) study the importance of covariates in their model and demonstrate that predicting BA, no other variables except CNT have a significant effect, and vice versa. Hence, we are not including the other variables except the locations as covariates in our analysis. To assess spatial dependence, we plot empirical semivariograms of residuals obtained by separately regressing  $\log(1 + \text{BA}(\mathbf{s}))$  and  $\log(1 + \text{CNT}(\mathbf{s}))$  on the covariates  $[1, \text{lon}(\mathbf{s}), \text{lat}(\mathbf{s})]^\top$ . The estimated range parameters  $\phi$  for burnt area and count responses are 2.622 and 2.646, respectively, values that are reasonably consistent with the separability assumption. We fix the smoothness parameter  $\nu = 0.3$ , as suggested by the fitted variograms, for subsequent analysis.

The spatial variability pattern of the residuals of  $\log(1 + \text{BA}(\mathbf{s}))$  and  $\log(1 + \text{CNT}(\mathbf{s}))$  in Figure 3 clearly illustrates that our proposed model may be a good fit. We present the estimation summary of real data analysis of our model ( $\mathcal{M}_1$ ) and the two competing models ( $\mathcal{M}_2, \mathcal{M}_3$ ) in Table 6. No spatially varying covariates among latitude or longitude, except the intercept, are statistically significant based on 95% posterior credible intervals. The resulting posterior mean of  $\Sigma$  from our model reveals the potential high correlations among the two types of components. The posterior credible interval of  $\Sigma_{12}$  in Table 7 does not contain zero. Therefore, the cross-covariance parameter is significantly greater than zero, which is well captured through our posterior analysis from  $\mathcal{M}_1$  and  $\mathcal{M}_3$ , while ignoring it in  $\mathcal{M}_2$ . Thus, Table 2 and Table 3 give substantial evidence of implementing our proposed model when the mixed-type multivariate responses in a scientific study are dependent. In Table 6, we also observe a high spatial correlation in the joint posterior random effect matrix  $\mathbf{W}$ , among the two components of log-transformed burnt areas and the count of

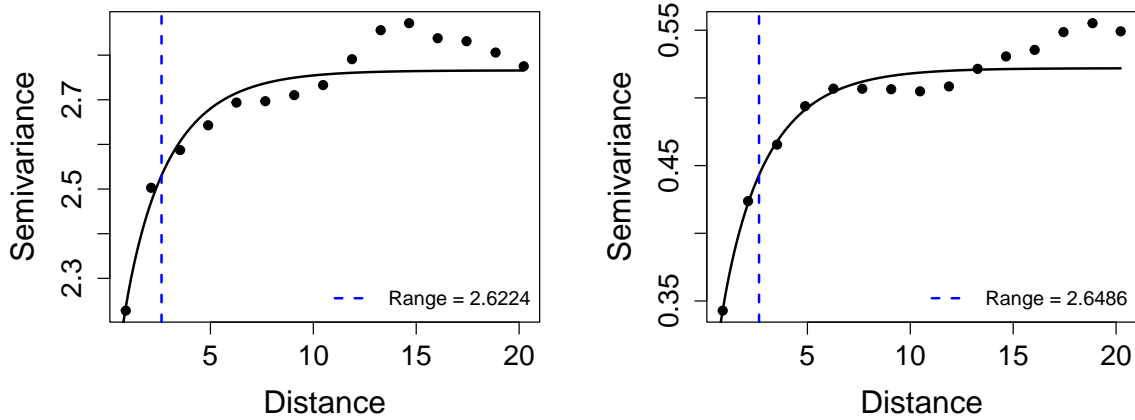


**Figure 3:** Semivariogram of residuals  $\log(1 + \text{BA})$  (left) and  $\log(1 + \text{CNT})$  (right) regression on locations as covariates for the dataset in September 2012.

wildfires. It significantly affects the quality of prediction, as demonstrated in Table 7. Since the prior effect is significant for  $\phi$  in the truncated domain, the estimated  $\phi$  is not close to what we obtain from semivariograms of the residuals of the fitted linear regression model. We perform a 5-fold cross-validation on a randomly split complete dataset and compute the WAIC and ELPD from the held-out locations to compare the joint bivariate model and separate univariate models for two different responses. We summarize our findings in Table 7 to check the prediction efficacy of our model  $\mathcal{M}_1$  with competing models  $\mathcal{M}_2$  and  $\mathcal{M}_3$ . We observe that, in all cases, our model outperforms the competing models in both measures. This highlights that, in the presence of dependence across responses, accounting for this cross-dependence, in addition to model fit, also improves prediction accuracy. Since our joint model enhances predictability with lower uncertainty, resource allocations across and within states can be optimized, leading to more effective wildfire management.

## 6 Discussions

We propose a novel joint Bayesian hierarchical model for high-dimensional spatial data with mixed-type responses. This framework captures the cross-dependence among different response types and the spatial dependence across the domain. To our knowledge, this is the first model that simultaneously offers flexibility, interpretability, and computational scalability. Unlike the `GPvecchia` package in R (Katzfuss and Guinness, 2021), which does not extend to multivariate Gaussian approximation, our method can be used by modeling a

**Table 6:** Posterior mean summary with 95% posterior credible intervals on full data set (\*posterior means of  $\phi$  appear twice for separate model, corresponding to the two components).

Parameters	$\mathcal{M}_1$	$\mathcal{M}_2$	$\mathcal{M}_3$
$\mathbf{B}_{11}$	−2.52 (−6.56, 1.16)	−1.99 (−5.00, 1.22)	−2.17 (−7.48, 3.65)
$\mathbf{B}_{12}$	−3.52 (−11.22, 3.33)	−4.42 (−10.13, 0.53)	−0.80 (−3.42, 2.08)
$\mathbf{B}_{21}$	−0.03 (−0.06, 0.01)	−0.02 (−0.05, 0.01)	−0.02 (−0.07, 0.03)
$\mathbf{B}_{22}$	−0.02 (−0.09, 0.04)	−0.03 (−0.08, 0.02)	−0.01 (−0.03, 0.02)
$\mathbf{B}_{31}$	0.02 (−0.02, 0.07)	0.02 (−0.03, 0.06)	0.02 (−0.05, 0.09)
$\mathbf{B}_{32}$	0.02 (−0.07, 0.11)	0.03 (−0.04, 0.10)	0.00 (−0.03, 0.04)
$\boldsymbol{\Sigma}_{11}$	0.83 ( 0.03, 1.71)	0.96 ( 0.08, 1.57)	1.58 ( 0.03, 3.45)
$\boldsymbol{\Sigma}_{12}$	1.44 ( 0.01, 3.00)	− (−)	0.74 ( 0.01, 1.61)
$\boldsymbol{\Sigma}_{22}$	2.82 ( 0.05, 5.78)	1.85 ( 0.05, 3.99)	0.39 ( 0.02, 0.81)
$\phi$	24.34 (16.32, 25.08)	10.10 ( 1.61, 24.36) 13.98 ( 4.32, 24.73)	24.46 (16.56, 25.09)

**Table 7:** Performances of all models based on WAIC, ELPD, and coverage with (SE).

Model	WAIC	ELPD (SE)	Coverage (SE)
$\mathcal{M}_1$	<b>40067.19</b>	<b>−4.892(0.061)</b>	0.9566(0.002)
$\mathcal{M}_2$	41182.48	−4.924(0.056)	0.9529(0.002)
$\mathcal{M}_3$	40735.11	−4.912(0.058)	0.9619(0.002)

sparsity-aware approximation of a multivariate latent spatial random effect with a separable covariance structure. Our approach enables fully Bayesian inference in high-dimensional spatial settings, making it particularly well-suited for modeling spatially indexed point process data over large and complex geographical regions. In contrast, traditional univariate process models fail to account for cross-response correlations, as demonstrated in our simulation-based predictive analysis. To ensure computational efficiency, we impose a sparse structure on the Cholesky factor of the precision matrix via the Vecchia approximation. Additionally, we incorporate an elliptical slice sampler for the latent GP and a blocked Gibbs sampler for the regression and cross-covariance matrices, which improves the mixing and convergence of the MCMC algorithm. However, there are methodologies for mixed-type response non-Gaussian spatial data (Zhang et al., 2023a) and spatio-temporal data (Pan et al., 2024) that bypass the MCMC algorithm, providing a faster method using Bayesian predictive stacking. Another domain of interest could be analyzing model selection for mixed-type multivariate spatial data, as in Ghosh and Deshpande (2025), a recent work in a non-spatial setup.

We have also established key theoretical properties of the model, including identifiability, a known challenge in non-replicated multivariate spatial settings. In our real-data application, we analyzed US wildfire data over 3503 spatial locations, demonstrating that our model consistently outperforms independent univariate process models. This superiority is evident through standard Bayesian model comparison metrics such as WAIC and ELPD. The EVA 2021 data challenge, however, involves spatio-temporal data with multiple land cover and meteorological variables; several avenues can also be explored to extend our model to temporally replicated spatial data (Zhu et al., 2005), spatio-temporal data (Zhang et al., 2023b), or in Bayesian model selection. While our current model assumes spatial isotropy, extending it to nonstationary settings presents a substantial challenge. In particular, modeling with non-separable covariance structures often leads to severe over-parameterization and identifiability issues (Genton and Kleiber, 2015), especially in the absence of temporally replicated data. Future work could explore scalable approximations to the high-dimensional posterior of the latent GP, such as domain partitioning or approximate Bayesian fusion (Dai et al., 2023) within the mixed-type response modeling framework.

## References

Bachoc, F., Porcu, E., Bevilacqua, M., Furrer, R., and Faouzi, T. (2022). Asymptotically equivalent prediction in multivariate geostatistics. *Bernoulli*, 28(4):2518–2545.

Bradley, J. R. and Clinch, M. (2025). Generating independent replicates directly from the posterior distribution for a class of spatial hierarchical models. *Journal of Computational and Graphical Statistics*, 34(1):123–139.

Brook, R. D., Rajagopalan, S., Pope III, C. A., Brook, J. R., Bhatnagar, A., Diez-Roux, A. V., Holguin, F., Hong, Y., Luepker, R. V., Mittleman, M. A., et al. (2010). Particulate matter air pollution and cardiovascular disease: an update to the scientific statement from the American heart association. *Circulation*, 121(21):2331–2378.

Burnett, R., Chen, H., Szyszkowicz, M., Fann, N., Hubbell, B., Pope III, C. A., Apte, J. S., Brauer, M., Cohen, A., Weichenthal, S., et al. (2018). Global estimates of mortality associated with long-term exposure to outdoor fine particulate matter. *Proceedings of the National Academy of Sciences*, 115(38):9592–9597.

Christensen, O. Roberts, G. and Sköld, M. (2006). Robust Markov chain Monte Carlo methods for spatial generalized linear mixed models. *Journal of Computational and Graphical Statistics*, 15(1):1–17.

Cisneros, D., Gong, Y., Yadav, R., Hazra, A., and Huser, R. (2023). A combined statistical and machine learning approach for spatial prediction of extreme wildfire frequencies and sizes. *Extremes*, 26(2):301–330.

Cooper, A., Vehtari, A., and Forbes, C. (2025). Joint leave-group-out cross-validation in Bayesian spatial models. *arXiv preprint arXiv:2504.15586*.

Cotter, S. L., Roberts, G. O., Stuart, A. M., and White, D. (2013). MCMC methods for functions: modifying old algorithms to make them faster. *Statistical Science*, 28(3).

Dai, H., Pollock, M., and Roberts, G. O. (2023). Bayesian fusion: Scalable unification of distributed statistical analyses. *Journal of the Royal Statistical Society Series B: Statistical Methodology*, 85(1):84–107.

de Leon, A. R. and Wu, B. (2011). Copula-based regression models for a bivariate mixed discrete and continuous outcome. *Statistics in Medicine*, 30(2):175–185.

Diggle, P. J., Tawn, J. A., and Moyeed, R. A. (1998). Model-based geostatistics. *Journal of the Royal Statistical Society Series C: Applied Statistics*, 47(3):299–350.

Ekvall, K. O. and Molstad, A. J. (2022). Mixed-type multivariate response regression with covariance estimation. *Statistics in Medicine*, 41(15):2768–2785.

Fitzmaurice, G. M. and Laird, N. M. (1995). Regression models for a bivariate discrete and continuous outcome with clustering. *Journal of the American Statistical Association*, 90(431):845–852.

Genton, M. G. and Kleiber, W. (2015). Cross-Covariance Functions for Multivariate Geostatistics. *Statistical Science*, 30(2):147 – 163.

Ghosh, S. and Deshpande, S. K. (2025). High-dimensional regression with outcomes of mixed-type using the multivariate spike-and-slab lasso. *arXiv preprint arXiv:2506.13007*.

Goldstein, H., Carpenter, J., Kenward, M., and Levin, K. (2009). Multilevel models with multivariate mixed response types. *Statistical Modelling*, 9(3):173–197.

Gueorguieva, R. (2001). A multivariate generalized linear mixed model for joint modelling of clustered outcomes in the exponential family. *Statistical Modelling*, 1(3):177–193.

Guinness, J. (2018). Permutation and grouping methods for sharpening Gaussian process approximations. *Technometrics*, 60(4):415–429.

Hazra, A. and Huser, R. (2021). Estimating high-resolution red sea surface temperature hotspots, using a low-rank semiparametric spatial model. *The Annals of Applied Statistics*, 15(2):572–596.

Hazra, A., Huser, R., and Bolin, D. (2024). Efficient modeling of spatial extremes over large geographical domains. *Journal of Computational and Graphical Statistics*.

Hazra, A., Reich, B. J., and Staicu, A.-M. (2020). A multivariate spatial skew-t process for joint modeling of extreme precipitation indexes. *Environmetrics*, 31(3):e2602.

Iglesias, V., Balch, J. K., and Travis, W. R. (2022). US fires became larger, more frequent, and more widespread in the 2000s. *Science Advances*, 8(11).

Jiryaei, F., N., W., de Leon, A. R., and Wu, B. (2016). Gaussian copula distributions for mixed data, with application in discrimination. *Journal of Statistical Computation and Simulation*, 86(9):1643–1659.

Kassahun, W., Neyens, T., Molenberghs, G., Faes, C., and Verbeke, G. (2015). A joint model for hierarchical continuous and zero-inflated overdispersed count data. *Journal of Statistical Computation and Simulation*, 85(3):552–571.

Katzfuss, M. and Guinness, J. (2021). A general framework for vecchia approximations of Gaussian processes. *Statistical Science*, 36(1):124–141.

Matern, B. (1960). *Spatial Variations (1st ed.)*. Berlin: Springer-Verlag.

Molenberghs, G., Verbeke, G., Demétrio, C. G. B., and Vieira, A. M. C. (2010). A family of generalized linear models for repeated measures with normal and conjugate random effects. *Statistical Science*, 25(3):325 – 347.

Murray, I., Adams, R., and MacKay, D. (2010). Elliptical slice sampling. In *Proceedings of the Thirteenth International Conference on Artificial Intelligence and Statistics*, pages 541–548. JMLR Workshop and Conference Proceedings.

Nandy, S., Holan, S. H., Bradley, J. R., and Wikle, C. K. (2022). Bayesian hierarchical models for multi-type survey data using spatially correlated covariates measured with error. *arXiv preprint arXiv:2211.09797*.

Opitz, T. (2023). Editorial: EVA-2021 data challenge on spatiotemporal prediction of wildfire extremes in the USA. *Extremes*, 26(16):241–250.

Pan, S., Zhang, L., Bradley, J. R., and Banerjee, S. (2024). Bayesian inference for spatial-temporal non-Gaussian data using predictive stacking. *arXiv preprint arXiv:2406.04655*.

Rudolf, D. and Sprungk, B. (2022). Robust random walk-like Metropolis-Hastings algorithms for concentrating posteriors. *arXiv preprint arXiv:2202.12127*.

Rue, H. and Martino, S. (2007). Approximate Bayesian inference for hierarchical Gaussian Markov random field models. *Journal of Statistical Planning and Inference*, 137(10):3177–3192.

Sammel, M. D., Ryan, L. M., and Legler, J. M. (1997). Latent variable models for mixed discrete and continuous outcomes. *Journal of the Royal Statistical Society: Series B (Methodological)*, 59(3):667–678.

Schafer, F., Katzfuss, M., and Owhadi, H. (2021). Sparse cholesky factorization by Kullback–Leibler minimization. *SIAM Journal on Scientific Computing*, 43(3):A2019–A2046.

Song, P. X.-K., Li, M., and Yuan, Y. (2009). Joint regression analysis of correlated data using Gaussian copulas. *Biometrics*, 65(1):60–68.

Stein, M. (1999). *Interpolation of Spatial Data: Some Theory for Kriging*. New York: Springer-Verlag.

Turner, M. C., Krewski, D., Pope III, C. A., Chen, Y., Gapstur, S. M., and Thun, M. J. (2011). Long-term ambient fine particulate matter air pollution and lung cancer in a large cohort of never-smokers. *American Journal of Respiratory and Critical Care Medicine*, 184(12):1374–1381.

Vecchia, A. V. (1988). Estimation and model identification for continuous spatial processes. *Journal of the Royal Statistical Society: Series B (Methodological)*, 50(2):297–312.

Yang, E., Ravikumar, P., Allen, G. I., Baker, Y., Wan, Y.-W., and Liu, Z. (2014). A general framework for mixed graphical models. *arXiv preprint arXiv:1411.0288*.

Zhang, H. (2004). Inconsistent estimation and asymptotically equal interpolations in model-based geostatistics. *Journal of the American Statistical Association*, 99(465):250–261.

Zhang, L., Banerjee, S., and Finley, A. O. (2021). High-dimensional multivariate geostatistics: A Bayesian matrix-normal approach. *Environmetrics*, 32(4):e2675.

Zhang, L., Tang, W., and Banerjee, S. (2023a). Bayesian geostatistics using predictive stacking. *arXiv preprint arXiv:2304.12414*.

Zhang, Z., Krainski, E., Zhong, P., Rue, H., and Huser, R. (2023b). Joint modeling and prediction of massive spatio-temporal wildfire count and burnt area data with the INLA-SPDE approach. *Extremes*, 26(2):339–351.

Zhou, S. and Bradley, J. R. (2024). Multiscale multi-type spatial Bayesian analysis of wildfires and population change that avoids MCMC and approximating the posterior distribution. *arXiv preprint arXiv:2410.02905*.

Zhu, J., Eickhoff, J. C., and Yan, P. (2005). Generalized linear latent variable models for repeated measures of spatially correlated multivariate data. *Biometrics*, 61(3):674–683.

## A Exponential family distributions

In Section 5, we consider Gaussian, Bernoulli, and Poisson responses. However, our spatial mixed-type model enables us to accommodate other well-known members of the exponential

**Table 8:** Exponential family distributions with canonical link functions

Distribution	Params	Canonical Link	$\psi$	$b(w)$	$h(y, \psi)$
Gaussian	$\mu, \sigma^2$	$w = \mu$	$\sigma^2$	$\frac{w^2}{2}$	$\frac{1}{\sqrt{2\pi\sigma^2}} \exp\left(-\frac{y^2}{2\sigma^2}\right)$
Bernoulli	$p$	$w = \log\left(\frac{p}{1-p}\right)$	1	$\log(1 + e^w)$	1
Poisson	$\lambda$	$w = \log(\lambda)$	1	$e^w$	$\frac{1}{y!}$
Binomial	$p, m$	$w = \log\left(\frac{p}{1-p}\right)$	1	$m \log(1 + e^w)$	$\binom{m}{y}$
Gamma	$\theta, \alpha$	$w = \frac{1}{\theta}$	$\alpha$	$-\log(-w)$	$\frac{y^{\alpha-1}}{\Gamma(\alpha)} \mathbf{1}_{\{y>0\}}$
Neg-Binomial	$p, r$	$w = \log\left(\frac{p}{1-p}\right)$	$r$	$-r \log(1 - e^w)$	$\binom{y+r-1}{y}$

family of distributions. Table 8 presents a list of well-known distributions along with their corresponding parameters.

## B Blocked-Gibbs sampler

We discuss a detailed derivation of the steps of the Matrix-Normal Inverse-Wishart (MNIW) Blocked-Gibbs sampler mentioned in Section 3. The prior density of the random effect matrix  $\mathbf{W}$  is given by,

$$\begin{aligned} \pi(\mathbf{W} \mid \mathbf{B}, \boldsymbol{\Sigma}, \phi) \\ = (2\pi)^{-nq/2} |\mathbf{K}_{\phi, (m)}|^{-q/2} |\boldsymbol{\Sigma}|^{-n/2} \exp\left\{-\frac{1}{2} \text{tr} \left[ \boldsymbol{\Sigma}^{-1} (\mathbf{W} - \mathbf{X}\mathbf{B})^\top \mathbf{K}_{\phi, (m)}^{-1} (\mathbf{W} - \mathbf{X}\mathbf{B}) \right] \right\}. \end{aligned}$$

Similarly the prior density of  $\boldsymbol{\Sigma}$  is given by,

$$\pi(\boldsymbol{\Sigma}) = \frac{1}{2^{vq/2} \Gamma(v/2)} |\mathbf{S}|^{v/2} |\boldsymbol{\Sigma}|^{-(v+q+1)/2} \exp\left\{-\frac{1}{2} \text{tr} \left\{ \mathbf{S} \boldsymbol{\Sigma}^{-1} \right\} \right\}.$$

The marginal posterior density of  $\boldsymbol{\Sigma} \mid \mathbf{W}, \phi, \mathbf{Y}$  is obtained by

$$\begin{aligned}\pi(\boldsymbol{\Sigma} \mid \mathbf{W}, \phi, \mathbf{Y}) &= \int \pi(\boldsymbol{\Sigma}, \mathbf{B} \mid \mathbf{W}, \phi, \mathbf{Y}) d\mathbf{B} \\ &= \int p(\mathbf{W} \mid \mathbf{B}, \boldsymbol{\Sigma}) \pi(\mathbf{B} \mid \mathbf{M}, \mathbf{V}, \boldsymbol{\Sigma}) \pi(\boldsymbol{\Sigma} \mid \mathbf{S}, v).\end{aligned}$$

In the blocked Gibbs sampler, instead of sampling from the full conditional posterior of  $\boldsymbol{\Sigma}$  given  $\mathbf{B} \mid \mathbf{W}, \phi, \mathbf{Y}$ , we integrate out  $\mathbf{B}$  and draw from the marginal full conditional posterior density  $\pi(\boldsymbol{\Sigma}, \mathbf{B} \mid \mathbf{W}, \phi, \mathbf{Y})$ . We outline the derivation of  $\pi(\boldsymbol{\Sigma}, \mathbf{B} \mid \mathbf{W}, \phi, \mathbf{Y})$  as given below

$$\begin{aligned}\pi(\boldsymbol{\Sigma}, \mathbf{B} \mid \mathbf{W}, \phi, \mathbf{Y}) &\propto |\mathbf{K}_{\phi, (m)}|^{-q/2} |\boldsymbol{\Sigma}|^{-n/2} \exp\left\{-\frac{1}{2} \operatorname{tr}[\boldsymbol{\Sigma}^{-1}(\mathbf{W} - \mathbf{X}\mathbf{B})^\top \mathbf{K}_{\phi, (m)}^{-1}(\mathbf{W} - \mathbf{X}\mathbf{B})]\right\} \\ &\quad \times |\mathbf{V}|^{-q/2} |\boldsymbol{\Sigma}|^{-p/2} \exp\left\{-\frac{1}{2} \operatorname{tr}[\boldsymbol{\Sigma}^{-1}(\mathbf{B} - \mathbf{M})^\top \mathbf{V}^{-1}(\mathbf{B} - \mathbf{M})]\right\} \\ &\quad \times |\boldsymbol{\Sigma}|^{-(v+q+1)/2} \exp\left\{-\frac{1}{2} \operatorname{tr}[\boldsymbol{\Sigma}^{-1}\mathbf{S}]\right\}.\end{aligned}$$

Substituting  $\tilde{\mathbf{V}} = (\mathbf{X}^\top \mathbf{K}_{\phi, (m)}^{-1} \mathbf{X} + \mathbf{V}^{-1})^{-1}$ ,  $\tilde{\mathbf{M}} = \tilde{\mathbf{V}}(\mathbf{X}^\top \mathbf{K}_{\phi, (m)}^{-1} \mathbf{W} + \mathbf{V}^{-1}\mathbf{M})$  in the joint full conditional posterior, we get the simplified expression below

$$\begin{aligned}\pi(\boldsymbol{\Sigma}, \mathbf{B} \mid \mathbf{W}, \phi, \mathbf{Y}) &\propto |\boldsymbol{\Sigma}|^{-(v+p+q+n+1)/2} \exp\left\{-\frac{1}{2} \operatorname{tr}[\boldsymbol{\Sigma}^{-1}(\mathbf{S} + \mathbf{W}^\top \mathbf{K}_{\phi, (m)}^{-1} \mathbf{W} + \mathbf{M}^\top \mathbf{V}^{-1} \mathbf{M} - \tilde{\mathbf{M}}^\top \tilde{\mathbf{V}}^{-1} \tilde{\mathbf{M}})]\right\} \\ &\propto |\boldsymbol{\Sigma}|^{-(v+p+q+n+1)/2} \exp\left\{-\frac{1}{2} \operatorname{tr}[\boldsymbol{\Sigma}^{-1}(\mathbf{B} - \tilde{\mathbf{M}})^\top \tilde{\mathbf{V}}^{-1}(\mathbf{B} - \tilde{\mathbf{M}})]\right\}.\end{aligned}\tag{20}$$

Integrating out the density of  $\mathbf{B}$  in (20) we obtain,

$$\boldsymbol{\Sigma} \mid \mathbf{W}, \phi \sim \mathcal{IW}_q(\tilde{\mathbf{S}} = \mathbf{S} + \mathbf{W}^\top \mathbf{K}_{\phi, (m)}^{-1} \mathbf{W} + \mathbf{M}^\top \mathbf{V}^{-1} \mathbf{M} - \tilde{\mathbf{M}}^\top \tilde{\mathbf{V}}^{-1} \tilde{\mathbf{M}}, \tilde{v} = v + n).$$

The full conditional distribution of  $\mathbf{B} \mid \Sigma, \phi, \mathbf{W}, \mathbf{Y}$  is obtained by

$$\begin{aligned}
& \pi(\mathbf{B} \mid \Sigma, \phi, \mathbf{W}, \mathbf{Y}) \\
& \propto p(\mathbf{W} \mid \mathbf{B}, \Sigma) \pi(\mathbf{B} \mid \mathbf{M}, \mathbf{V}, \Sigma) \\
& \propto (2\pi)^{-nq/2} |\mathbf{K}_{\phi, (m)}|^{-q/2} |\Sigma|^{-n/2} \exp \left\{ -\frac{1}{2} \text{tr} \left[ \Sigma^{-1} (\mathbf{W} - \mathbf{X}\mathbf{B})^\top \mathbf{K}_{\phi, (m)}^{-1} (\mathbf{W} - \mathbf{X}\mathbf{B}) \right] \right\} \\
& \quad \times (2\pi)^{-pq/2} |\mathbf{V}|^{-q/2} |\Sigma|^{-p/2} \exp \left\{ -\frac{1}{2} \text{tr} \left[ \Sigma^{-1} (\mathbf{B} - \mathbf{M})^\top \mathbf{V}^{-1} (\mathbf{B} - \mathbf{M}) \right] \right\} \\
& \propto \exp \left\{ -\frac{1}{2} \text{tr} \left[ \Sigma^{-1} (\mathbf{B}^\top \mathbf{X}^\top \mathbf{K}_{\phi, (m)}^{-1} \mathbf{X}\mathbf{B} - \mathbf{B}^\top \mathbf{X}^\top \mathbf{K}_{\phi, (m)}^{-1} \mathbf{W} - \mathbf{W}^\top \mathbf{K}_{\phi, (m)}^{-1} \mathbf{X}\mathbf{B} + \mathbf{W}^\top \mathbf{K}_{\phi, (m)}^{-1} \mathbf{W}) \right] \right\} \\
& \quad \times \exp \left\{ -\frac{1}{2} \text{tr} \left[ \Sigma^{-1} (\mathbf{B}^\top \mathbf{V}^{-1} \mathbf{B} - \mathbf{B}^\top \mathbf{V}^{-1} \mathbf{M} - \mathbf{M}^\top \mathbf{V}^{-1} \mathbf{B} + \mathbf{M}^\top \mathbf{V}^{-1} \mathbf{M}) \right] \right\} \\
& \propto \exp \left\{ -\frac{1}{2} \text{tr} \left[ \Sigma^{-1} (\mathbf{B}^\top (\mathbf{X}^\top \mathbf{K}_{\phi, (m)}^{-1} \mathbf{X} + \mathbf{V}^{-1}) \mathbf{B} - 2\mathbf{B}^\top (\mathbf{X}^\top \mathbf{K}_{\phi, (m)}^{-1} \mathbf{W} + \mathbf{V}^{-1} \mathbf{M})) \right] \right\} \\
& \propto \exp \left\{ -\frac{1}{2} \text{tr} \left[ \Sigma^{-1} (\mathbf{B} - \widetilde{\mathbf{M}})^\top \widetilde{\mathbf{V}}^{-1} (\mathbf{B} - \widetilde{\mathbf{M}}) \right] \right\}.
\end{aligned} \tag{21}$$

Given  $\Sigma, \phi, \mathbf{W}$ , we obtain the Matrix-Normal full conditional posterior of  $\mathbf{B}$  in (21) as  $\mathbf{B} \mid \Sigma, \phi, \mathbf{W} \sim \mathcal{MN}_{p,q}(\widetilde{\mathbf{M}}, \widetilde{\mathbf{V}}, \Sigma)$ .

## C Elliptical slice sampler

In this section, we outline the definition of the Matrix-Normal distribution and sampling procedure using the Cholesky factorization of the precision matrices, which is used in inference and prediction in our Algorithm 1.

**Definition 5.** A random matrix  $\mathbf{Z}_{m \times n}$  is said to follow a Matrix-Normal distribution with mean matrix  $\mathbf{M}$ , row-wise covariance being  $\mathbf{V}$  and column-wise covariance being  $\mathbf{U}$  and denoted by  $\mathbf{Z} \sim \mathcal{MN}_{m,n}(\mathbf{M}, \mathbf{U}, \mathbf{V})$  if its probability density function is given by

$$\pi(\mathbf{Z} \mid \mathbf{M}, \mathbf{U}, \mathbf{V}) = \frac{1}{(2\pi)^{mn/2} |\mathbf{U}|^{n/2} |\mathbf{V}|^{m/2}} \exp \left\{ -\frac{1}{2} \text{tr} [\mathbf{V}^{-1} (\mathbf{Z} - \mathbf{M})^\top \mathbf{U}^{-1} (\mathbf{Z} - \mathbf{M})] \right\},$$

where  $\mathbf{M}$  is an  $m \times n$  mean matrix,  $\mathbf{U}$  is an  $m \times m$  row covariance matrix, and  $\mathbf{V}$  is an  $n \times n$  column covariance matrix. Equivalently, if  $\mathbf{Z} \sim \mathcal{MN}_{m,n}(\mathbf{M}, \mathbf{U}, \mathbf{V})$ , then  $\text{vec}(\mathbf{Z}) \sim \mathcal{N}_{mn}(\text{vec}(\mathbf{M}), \mathbf{V} \otimes \mathbf{U})$ , where  $\otimes$  denotes the Kronecker product.

We now present the sampling from the Matrix-Normal density. Suppose  $\mathbf{X} \sim \mathcal{MN}_{m,n}(\mathbf{0}, \mathbf{I}_m, \mathbf{I}_n)$ . Let  $\mathbf{Y} = \mathbf{M} + \mathbf{A}\mathbf{X}\mathbf{B}^\top$ , then  $\mathbf{Y} \sim \mathcal{MN}_{m,n}(\mathbf{M}, \mathbf{U}^{-1}, \mathbf{V}^{-1})$ , where  $\mathbf{A} = \text{chol}(\mathbf{U}^{-1})$  and  $\mathbf{B} = \text{chol}(\mathbf{V}^{-1})$ , so that  $\mathbf{A}\mathbf{A}^\top = \mathbf{U}^{-1}$  and  $\mathbf{B}\mathbf{B}^\top = \mathbf{V}^{-1}$ .

---

**Algorithm 1** Elliptic Slice Sampler Update for  $\mathbf{W}$ 


---

**Require:**  $\mathbf{W}$ ,  $\mathbf{B}$ ,  $\mathbf{U}_\Sigma = \text{chol}(\Sigma^{-1})$ ,  $\mathbf{U}_{\phi,(m)} = \text{chol}(\mathbf{K}_{\phi,(m)}^{-1})$ ,  $\mathbf{Y}$ ,  $\mathbf{X}$ , family.

```

1: Sample  $\gamma \sim \text{Uniform}(0, 2\pi)$ 
2: Set  $\gamma_{\min} \leftarrow \gamma - 2\pi$ ,  $\gamma_{\max} \leftarrow \gamma$ 
3: Sample  $\mathbf{Z} \sim \mathcal{MN}_{n,q}(\mathbf{0}, \mathbf{I}_n, \mathbf{I}_q)$ 
4: Compute  $\mathbf{Z}_{\text{new}} \leftarrow \mathbf{Z}(\mathbf{U}_\Sigma^\top)^{-1}$ 
5: Compute prior draw:  $\mathbf{W}_{\text{prior}} \leftarrow \mathbf{U}_{\phi,(m)}^{-1} \mathbf{Z}_{\text{new}}$ 
6: Compute prior mean:  $\boldsymbol{\mu}_\mathbf{W} \leftarrow \mathbf{X}\boldsymbol{\beta}$ 
7: Compute current log-likelihood:  $\log L_{\text{curr}} \leftarrow \log L(\mathbf{W}, \mathbf{Y}, \text{family})$ 
8: repeat
9:   Propose candidate:
```

$$\mathbf{W}_{\text{cand}} \leftarrow \boldsymbol{\mu}_\mathbf{W} + (\mathbf{W} - \boldsymbol{\mu}_\mathbf{W}) \cos(\gamma) + \mathbf{W}_{\text{prior}} \sin(\gamma)$$

```

10:  Compute candidate log-likelihood:  $\log L_{\text{cand}} \leftarrow \log L(\mathbf{W}_{\text{cand}}, \mathbf{Y}, \text{family})$ 
11:  Compute acceptance ratio:  $\log r \leftarrow \log L_{\text{cand}} - \log L_{\text{curr}}$ 
12:  if  $\log u < \log r$  where  $u \sim \mathcal{U}(0, 1)$  then
13:    Accept:  $\mathbf{W} \leftarrow \mathbf{W}_{\text{cand}}$ ,  $\log L \leftarrow \log L_{\text{cand}}$ 
14:    break
15:  else
16:    if  $\gamma < 0$  then
17:       $\gamma_{\min} \leftarrow \gamma$ 
18:    else
19:       $\gamma_{\max} \leftarrow \gamma$ 
20:    end if
21:    Resample  $\gamma \sim \text{Uniform}(\gamma_{\min}, \gamma_{\max})$ 
22:  end if
23: until accepted
24: return Updated  $\mathbf{W}$ .
```

---

## D Posterior latent predictive process

In this section, we present the details for the density of the latent posterior predictive process, in the form of precision matrix parameterization (18) mentioned in Section 4. This parameterization of  $\mathcal{W}(\cdot)$  is a key component in drawing predictive samples using the sparse Vecchia approximation. Define  $\mathbf{W}^* = [\mathbf{W}(\mathbf{s}_1^*)^\top, \mathbf{W}(\mathbf{s}_2^*)^\top, \dots, \mathbf{W}(\mathbf{s}_u^*)^\top]^\top$  denote the latent predictive process and let  $\mathbf{X}^* = [\mathbf{X}(\mathbf{s}_1^*)^\top, \mathbf{X}(\mathbf{s}_2^*)^\top, \dots, \mathbf{X}(\mathbf{s}_u^*)^\top]^\top$  be the covariate over  $\mathcal{U}$ .

**Theorem 6.** Assume the joint distribution of  $[\mathbf{W}^{*\top}, \mathbf{W}^\top]^\top$  on  $\mathcal{U} \cup \mathcal{S}$  be

$$\begin{bmatrix} \mathbf{W}^* \\ \mathbf{W} \end{bmatrix} \sim \mathcal{MN}_{u+n, q} \left( \begin{bmatrix} \mathbf{X}^* \mathbf{B} \\ \mathbf{X} \mathbf{B} \end{bmatrix}, \mathbf{K}_{\phi, (m)}^{(u+n)} = \begin{bmatrix} \mathbf{K}_{\phi, (m)}^{(u,u)} & \mathbf{K}_{\phi, (m)}^{(u,n)} \\ \mathbf{K}_{\phi, (m)}^{(n,u)} & \mathbf{K}_{\phi, (m)}^{(n,n)} \end{bmatrix}, \Sigma \right).$$

The kriging equation (conditional distribution) of  $\mathbf{W}^*$  given  $\mathbf{W}$  is

$$\mathbf{W}^* \mid \mathbf{W}, \mathbf{B}, \Sigma, \phi \sim \mathcal{MN}_{u, q}(\mathbf{M}_{W*}, \mathbf{K}_{W*}, \Sigma), \quad (22)$$

with

$$\mathbf{M}_{W*} = \mathbf{X}^* \mathbf{B} + \mathbf{K}_{\phi, (m)}^{(u,n)} (\mathbf{K}_{\phi, (m)}^{(n,n)})^{-1} (\mathbf{W} - \mathbf{X} \mathbf{B}), \quad \mathbf{K}_{W*} = \mathbf{K}_{\phi, (m)}^{(u,u)} - \mathbf{K}_{\phi, (m)}^{(u,n)} (\mathbf{K}_{\phi, (m)}^{(n,n)})^{-1} \mathbf{K}_{\phi, (m)}^{(n,u)}.$$

Write the joint precision matrix  $\mathbf{Q}_{\phi, (m)}^{(u+n)} = (\mathbf{K}_{\phi, (m)}^{(u+n)})^{-1}$  partitioned conformably as

$$\mathbf{Q}_{\phi, (m)}^{(u+n)} = \begin{bmatrix} \mathbf{Q}_{\phi, (m)}^{(u,u)} & \mathbf{Q}_{\phi, (m)}^{(u,n)} \\ \mathbf{Q}_{\phi, (m)}^{(n,u)} & \mathbf{Q}_{\phi, (m)}^{(n,n)} \end{bmatrix}.$$

Then (22) can be written in the precision-block form

$$\mathbf{W}^* \mid \mathbf{W}, \mathbf{B}, \Sigma, \phi \sim \mathcal{MN}_{u, q} \left( \mathbf{X}^* \mathbf{B} - (\mathbf{Q}_{\phi, (m)}^{(u,u)})^{-1} \mathbf{Q}_{\phi, (m)}^{(u,n)} (\mathbf{W} - \mathbf{X} \mathbf{B}), (\mathbf{Q}_{\phi, (m)}^{(u,u)})^{-1}, \Sigma \right).$$

*Proof.* From the identity of  $\mathbf{K}_{\phi, (m)}^{(u+n)} \mathbf{Q}_{\phi, (m)}^{(u+n)} = \mathbf{I}_{u+n}$ , we multiply the block partitions as

$$\begin{bmatrix} \mathbf{K}_{\phi, (m)}^{(u,u)} & \mathbf{K}_{\phi, (m)}^{(u,n)} \\ \mathbf{K}_{\phi, (m)}^{(n,u)} & \mathbf{K}_{\phi, (m)}^{(n,n)} \end{bmatrix} \begin{bmatrix} \mathbf{Q}_{\phi, (m)}^{(u,u)} & \mathbf{Q}_{\phi, (m)}^{(u,n)} \\ \mathbf{Q}_{\phi, (m)}^{(n,u)} & \mathbf{Q}_{\phi, (m)}^{(n,n)} \end{bmatrix} = \begin{bmatrix} \mathbf{I}_u & \mathbf{0} \\ \mathbf{0} & \mathbf{I}_n \end{bmatrix}.$$

Equating blocks yields

$$\mathbf{K}_{\phi, (m)}^{(u,u)} \mathbf{Q}_{\phi, (m)}^{(u,u)} + \mathbf{K}_{\phi, (m)}^{(u,n)} \mathbf{Q}_{\phi, (m)}^{(n,u)} = \mathbf{I}_u, \quad (23)$$

$$\mathbf{K}_{\phi, (m)}^{(u,u)} \mathbf{Q}_{\phi, (m)}^{(u,n)} + \mathbf{K}_{\phi, (m)}^{(u,n)} \mathbf{Q}_{\phi, (m)}^{(n,n)} = \mathbf{0}_{u \times n}, \quad (24)$$

$$\mathbf{K}_{\phi, (m)}^{(n,u)} \mathbf{Q}_{\phi, (m)}^{(u,u)} + \mathbf{K}_{\phi, (m)}^{(n,n)} \mathbf{Q}_{\phi, (m)}^{(n,u)} = \mathbf{0}_{n \times u}, \quad (25)$$

$$\mathbf{K}_{\phi, (m)}^{(n,u)} \mathbf{Q}_{\phi, (m)}^{(u,n)} + \mathbf{K}_{\phi, (m)}^{(n,n)} \mathbf{Q}_{\phi, (m)}^{(n,n)} = \mathbf{I}_n. \quad (26)$$

We express  $\mathbf{Q}_{\phi,(m)}^{(n,u)}$  via  $\mathbf{Q}_{\phi,(m)}^{(u,u)}$ . From (25) we get  $\mathbf{K}_{\phi,(m)}^{(n,n)} \mathbf{Q}_{\phi,(m)}^{(n,u)} = -\mathbf{K}_{\phi,(m)}^{(n,u)} \mathbf{Q}_{\phi,(m)}^{(u,u)}$ . Assuming  $\mathbf{K}_{\phi,(m)}^{(n,n)}$  invertible (the usual predictive assumption), left-multiply by  $(\mathbf{K}_{\phi,(m)}^{(n,n)})^{-1}$  to obtain

$$\mathbf{Q}_{\phi,(m)}^{(n,u)} = -(\mathbf{K}_{\phi,(m)}^{(n,n)})^{-1} \mathbf{K}_{\phi,(m)}^{(n,u)} \mathbf{Q}_{\phi,(m)}^{(u,u)}.$$

Define the Schur's complement  $\mathbf{S}_{\phi,(m)} := \mathbf{K}_{\phi,(m)}^{(u,u)} - \mathbf{K}_{\phi,(m)}^{(u,n)} (\mathbf{K}_{\phi,(m)}^{(n,n)})^{-1} \mathbf{K}_{\phi,(m)}^{(n,u)}$ . We next derive the inverse of Schur's complement  $\mathbf{Q}_{\phi,(m)}^{(u,u)} = (\mathbf{S}_{\phi,(m)})^{-1}$ . Substitute the expression for  $\mathbf{Q}_{\phi,(m)}^{(n,u)}$  into (23) as  $\mathbf{K}_{\phi,(m)}^{(u,u)} \mathbf{Q}_{\phi,(m)}^{(u,u)} - \mathbf{K}_{\phi,(m)}^{(u,n)} (\mathbf{K}_{\phi,(m)}^{(n,n)})^{-1} \mathbf{K}_{\phi,(m)}^{(n,u)} \mathbf{Q}_{\phi,(m)}^{(u,u)} = \mathbf{I}_u$ . and factor the left-hand side to get

$$(\mathbf{K}_{\phi,(m)}^{(u,u)} - \mathbf{K}_{\phi,(m)}^{(u,n)} (\mathbf{K}_{\phi,(m)}^{(n,n)})^{-1} \mathbf{K}_{\phi,(m)}^{(n,u)}) \mathbf{Q}_{\phi,(m)}^{(u,u)} = \mathbf{I}_u. \quad (27)$$

From (27) we obtain  $\mathbf{S}_{\phi,(m)} \mathbf{Q}_{\phi,(m)}^{(u,u)} = \mathbf{I}_u \implies \mathbf{Q}_{\phi,(m)}^{(u,u)} = (\mathbf{S}_{\phi,(m)})^{-1}$ , which immediately gives  $\mathbf{K}_{W*} = \mathbf{S}_{\phi,(m)} = (\mathbf{Q}_{\phi,(m)}^{(u,u)})^{-1}$ . Next we express  $\mathbf{K}_{\phi,(m)}^{(u,n)} (\mathbf{K}_{\phi,(m)}^{(n,n)})^{-1}$  via  $\mathbf{Q}_{\phi,(m)}^{(u+n)}$  blocks. From (24) rearrange to  $\mathbf{K}_{\phi,(m)}^{(u,u)} \mathbf{Q}_{\phi,(m)}^{(u,n)} = -\mathbf{K}_{\phi,(m)}^{(u,n)} \mathbf{Q}_{\phi,(m)}^{(n,n)}$ . Left-multiply by  $(\mathbf{S}_{\phi,(m)})^{-1} = \mathbf{Q}_{\phi,(m)}^{(u,u)}$  and a direct algebraic simplification yields  $\mathbf{Q}_{\phi,(m)}^{(u,n)} = -(\mathbf{S}_{\phi,(m)})^{-1} \mathbf{K}_{\phi,(m)}^{(u,n)} (\mathbf{K}_{\phi,(m)}^{(n,n)})^{-1}$ . Rearranging this gives

$$\mathbf{K}_{\phi,(m)}^{(u,n)} (\mathbf{K}_{\phi,(m)}^{(n,n)})^{-1} = -\mathbf{Q}_{\phi,(m)}^{(u,u)-1} \mathbf{Q}_{\phi,(m)}^{(u,n)}.$$

Substitute into  $\mathbf{M}_{W*}$  and use the second identity in the covariance-form predictive mean

$$\mathbf{M}_{W*} = \mathbf{X}^* \mathbf{B} + \mathbf{K}_{\phi,(m)}^{(u,n)} (\mathbf{K}_{\phi,(m)}^{(n,n)})^{-1} (\mathbf{W} - \mathbf{X} \mathbf{B}) = \mathbf{X}^* \mathbf{B} - (\mathbf{Q}_{\phi,(m)}^{(u,u)})^{-1} \mathbf{Q}_{\phi,(m)}^{(u,n)} (\mathbf{W} - \mathbf{X} \mathbf{B}),$$

which matches the precision-form mean. Using the first identity, we have  $\mathbf{K}_{W*} = (\mathbf{Q}_{\phi,(m)}^{(u,u)})^{-1}$ , so the row-covariances agree. The column-covariance remains  $\Sigma$ . We consequently prove that the covariance-form predictive expression in (17) is equivalent to the stated precision-block representation.  $\square$